Acta Pharmaceutica Sinica B 2020;10(3):512–528

Chinese Pharmaceutical Association
Institute of Materia Medica, Chinese Academy of Medical Sciences

Acta Pharmaceutica Sinica B

www.elsevier.com/locate/apsb
www.sciencedirect.com

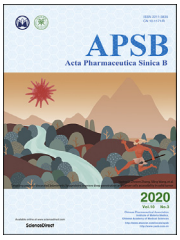

ORIGINAL ARTICLE

Synthesis and biological evaluation of a series of 2-(((5-akly/aryl-1*H*-pyrazol-3-yl)methyl)thio)-5-alkyl-6-(cyclohexylmethyl)-pyrimidin-4(3*H*)-ones as potential HIV-1 inhibitors

Yumeng Wu[a,†], Chengrun Tang[b,d,†], Ruomei Rui[a], Liumeng Yang[b], Wei Ding[a], Jiangyuan Wang[a], Yiming Li[a], Christopher C. Lai[c], Yueping Wang[a], Ronghua Luo[b], Weilie Xiao[a], Hongbing Zhang[a,*], Yongtang Zheng[b,*], Yanping He[a,*]

[a]*Key Laboratory of Medicinal Chemistry for Natural Resources, Ministry of Education and Yunnan Province, School of Chemical Science and Technology, Yunnan University, Kunming 650091, China*
[b]*Key Laboratory of Bioactive Peptides of Yunnan Province/Key Laboratory of Animal Models and Human Disease Mechanisms of the Chinese Academy of Sciences, the National Kunming High Level Biosafety Research Center for Nonhuman Primate, KIZ-CUHK Joint Laboratory of Bioresources and Molecular Research in Common Diseases, Kunming Institute of Zoology, Chinese Academy of Sciences, Kunming 650223, China*
[c]*Chemical Biology Laboratory, Center for Cancer Research, National Cancer Institute, National Institutes of Health, Frederick, MD 21702, USA*
[d]*School of Pharmaceutical Science & Yunnan Key Laboratory of Pharmacology for Natural Products, Kunming Medical University, Kunming 650500, China*

Received 6 June 2019; received in revised form 6 August 2019; accepted 22 August 2019

KEY WORDS

HIV-1;
NNRTIs;
S-DABOs;
Antiviral activity;
SAR;
Molecular modeling

Abstract A series of 2-(((5-akly/aryl-1*H*-pyrazol-3-yl)methyl)thio)-5-alkyl-6-(cyclohexylmethyl)-pyrimidin-4(3*H*)-ones were synthesized and their anti-HIV-1 activities were evaluated. Most of these compounds were highly active against wild-type (WT) HIV-1 strain (IIIB) with EC_{50} values in the range of 0.0038–0.4759 μmol/L. Among those compounds, **I-11** had an EC_{50} value of 3.8 nmol/L and SI (selectivity index) of up to 25,468 indicating excellent activity against WT HIV-1. *In vitro* anti-HIV-1 activity and resistance profile studies suggested that compounds **I-11** and **I-12** displayed potential anti-HIV-1 activity against laboratory adapted strains and primary isolated strains including different subtypes and

*Corresponding authors. Tel./ fax: +86 871 65035538.
E-mail addresses: yphe@ynu.edu.cn (Yanping He), zhengyt@mail.kiz.ac.cn (Yongtang Zheng), zhanghb@ynu.edu.cn (Hongbing Zhang).
†These authors made equal contributions to this work.
Peer review under responsibility of Institute of Materia Medica, Chinese Academy of Medical Sciences and Chinese Pharmaceutical Association.

https://doi.org/10.1016/j.apsb.2019.08.009
2211-3835 © 2020 Chinese Pharmaceutical Association and Institute of Materia Medica, Chinese Academy of Medical Sciences. Production and hosting by Elsevier B.V. This is an open access article under the CC BY-NC-ND license (http://creativecommons.org/licenses/by-nc-nd/4.0/).

tropism strains (EC_{50}s range from 4.3 to 63.6 nmol/L and 18.9−219.3 nmol/L, respectively). On the other hand, it was observed that those two compounds were less effective with EC_{50} values of 2.77 and 4.87 μmol/L for HIV-$1A_{17}$ (K103N + Y181C). The activity against reverse transcriptase (RT) was also evaluated for those compounds. Both **I-11** and **I-12** obtained sub-micromolar IC_{50} values showing their potential in RT inhibition. The pharmacokinetics examination in rats indicated that compound **I-11** has acceptable pharmacokinetic properties and bioavailability. Preliminary structure−activity relationships and molecular modeling studies were also discussed.

© 2020 Chinese Pharmaceutical Association and Institute of Materia Medica, Chinese Academy of Medical Sciences. Production and hosting by Elsevier B.V. This is an open access article under the CC BY-NC-ND license (http://creativecommons.org/licenses/by-nc-nd/4.0/).

1. Introduction

Non-nucleoside reverse transcriptase inhibitors (NNRTIs) are indispensable component of highly active antiretroviral therapy (HAART) that is widely used in the clinical treatment of HIV-1-infected patients[1−3]. Currently, five NNRTIs have been approved for clinical use: nevirapine (NVP), delavirdine (DLV), efavirenz (EFV), etravirine (ETR, TMC125), and rilpivirine (RPV, TMC278)[4,5]. However, therapeutic effectiveness of these available drugs has been limited to a certain extent by the emergence of drug-resistant viruses and potentially severe side effects with long-term clinical use[6−8]. As a result, discovery of novel NNRTIs candidates with better resistance profiles and improved safety and tolerability is a continuous goal of drug development[9−13].

Among NNRTIs of clinical interest, 2-alkylsulfanyl-6-benzyl-3,4-dihydropyrimidin-4(3*H*)-ones (*S*-DABOs) occupy a significant place for their unique antiviral potency, high specificity and low toxicity[14−16]. Studies on *S*-DABOs suggested that an alkyl/arylthio substituent at the C2 position, an aromatic ring linked through a methlyene bridge to the C6 position and the unmodified NHCO fragment constituting the N3 and C4 positions of the prymidine ring are structural determinants for the antiviral activity of these compounds[17−20]. The key interactions of *S*-DABOs with HIV-1 reverse transcriptase (RT) residues could be summarized as Fig. 1.

Previous research efforts in our lab led to the identification of a series of oxophenethyl-*S*-DABOs derivatives with significant anti-HIV-1 activity[21−24]. Especially, by replacing the C6-arylring with a C6-cyclohexylmethyl moiety, a new series oxophenethyl-*S*-DACOs of NNRTIs with higher potent and specificity was obtained[25]. The most promising compound **DB02** exhibited potent anti-HIV-1 activity against laboratory adapted strains and primary isolated strains (EC_{50}s (concentrations inhibiting virus replication by 50%) range from 2.40 to 41.8 nmol/L), along with an improved sensitivity against K103N or Y181C than *S*-DABOs[26]. The molecular modeling study (Fig. 1) indicated that the carbonyl oxygen of C2 side chain of **DB02** forms a key H-bond with the backbone (−NH− group) of K103 of HIV-1 RT which acts as essential

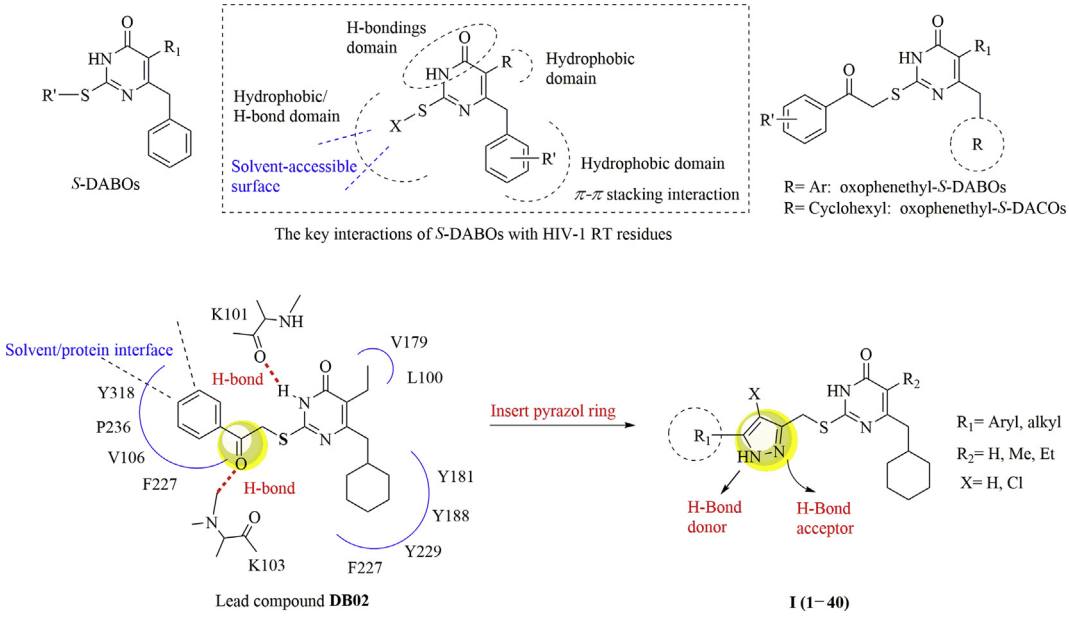

Figure 1 Structures of *S*-DABOs and newly designed compounds.

pharmacophore elements favorably contributing to ligand binding[26,27]. Since the ω-phenyl of C2 side chain point at the interface between the enzyme and the solvent, we could conclude that longer and diverse groups are tolerant of this region. The proposed binding mode for **DB02** allowed us to anticipate that the introduction of a pyrazol group, which contains both hydrogen bond donor and acceptor, at C2 side chain instead of a carbonyl group might further strengthen the hydrogen interactions with K103 of the viral enzyme RT. This could result in an improved potency against the wild-type or mutant HIV-1 strains. Meanwhile, to develop $\pi-\pi$ stack and van der Waals' interactions with the amino residues in this hydrophobic region around the C2 side chain, different substituents varying in their size and electronic nature were introduced to the C5′ and C3′ position of the pyrazol ring. Thus, a series of novel 2-(((5-akly/aryl-1*H*-pyrazol-3-yl)me-thyl) thio)-5-alkyl-6-(cyclohexylmethyl)-pyrimidin-4(3*H*)-one derivatives were designed based on the analysis of the ligand−receptor interactions (Fig. 1). In the newly designed analogs, different substituents varying in size and electronic nature were introduced to the ω-phenyl of C2 side chain located at the protein-solvent interface region of RT to further investigate the potential interaction. In this paper, we report the synthesis of this novel *S*-DACOs, the evaluation of their anti-HIV-1 activity and the structure−activity relationship (SAR) study in detail.

2. Results and discussion

2.1. Chemistry

The target compounds **I (1−40)** were prepared in a convergent manner by coupling two subunits as depicted in Scheme 1. Following the procedure described previously[21,25], the key intermediate β-ketoesters **3** were prepared by exposure of 2-cyclohexylacetic acid **1** to 1,1′-carbonyl-diimidazole (CDI) followed by treatment with different ethyl potassium malonates in the presence of anhydrous $MgCl_2$ and Et_3N[28]. Condensation of **3** with thiourea in the presence of EtONa in refluxing EtOH led to substituted uracil **4** which was subjected to *S*-alkylation in anhydrous DMF with 3-(bromomethyl)-5-R_1-1*H*-pyrazole (**10**) in the presence of K_2CO_3 to afford the target compounds **I (1−40)**. **10** required for the *S*-alkylation was prepared from appropriate methyl ketones **5**. The addition of methyl ketones **5** to diethyl malonate, followed by the cyclization with hydrazine for the pyrazole ring formation under refluxing condition gave the desired 5-substituted-1*H*-pyrazole-3-carboxylate (**7**) over two steps[29,30]. Halogenation on the pyrazole with NCS produced chlorinated pyrazole **8** in good yield. The ester moiety was then converted into the alcohol **9** by reduction with $LiAlH_4$ and then bromination with PBr_3 or Br_2 reagent. These synthesized compounds were characterized by physicochemical and spectral means. MS, ^{1}H NMR, ^{13}C NMR spectral data were found in agreement with the assigned molecular structures.

2.2. Anti-HIV-1 activity evaluation

The novel *S*-DACO derivatives **I (1−40)** were tested for their cytotoxicity and anti-HIV-1 activity in C8166 cells infected by the HIV-1_{IIIB} and compared with nevirapine (NVP), etravirine (ETR) and zidovudine (AZT). The activity data was interpreted in CC_{50} (concentration resulting in 50% cell death) values (cytotoxicity), EC_{50} (anti-HIV-1 activity) and SI (selectivity index, given by the CC_{50}/EC_{50} ratio) (Table 1). As another control, previously reported compound **DB02**[25,26] was included in our test assays for comparison.

As shown in Table 1, most of the target molecules exhibited good to excellent anti-HIV-1 (WT, wild-type) activity with EC_{50} ranging from 0.0038 to 0.4759 μmol/L except for compounds **I-38**, **I-39** and **I-40** with EC_{50}s of 4.9825, 3.9567 and

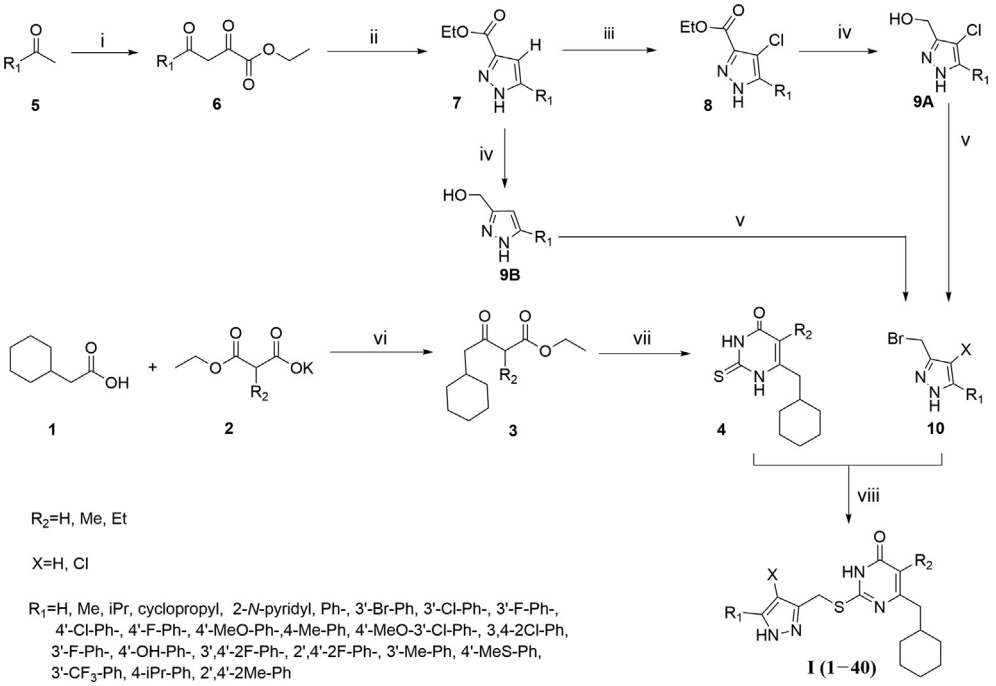

Scheme 1 Synthesis of compounds **I (1−40)**. Reagents and conditions: (i) diethyl malonate, EtONa, rt, 14 h; (ii) hydrazine hydrate, EtOH, reflux, 3 h; (iii) NCS, CH_3CN, DMF, 55 °C, 15 h; (iv) $LiAlH_4$, THF, 0 °C, 3 h; (v) PBr_3, or $(Ph)_3P$, Br_2 CH_3CN, reflux, or rt, 2 h; (vi) (a) $MgCl_2$, Et_3N, CH_3CN, rt, 2 h; (b) CDI, rt, overnight then reflux, 2 h; (vii) thiourea, EtONa, EtOH, reflux, 6 h; (viii) DMF, K_2CO_3, rt, 3−12 h.

Table 1 Activity against HIV-1_{IIIB} strain, cytotoxicity and SI of the title compounds in C8166 cells[a].

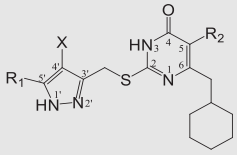

I (1–40)

Compd.	R_1	R_2	X	EC_{50}[b] (μmol/L)	CC_{50}[c] (μmol/L)	SI[d]
I-01	Ph	Et	H	0.0068 ± 0.0017	84.48 ± 0.91	12,424
I-02	3′-Me-Ph	Et	H	0.0739 ± 0.0079	82.76 ± 2.20	1120
I-03	3′-Br-Ph	Et	H	0.0512 ± 0.0073	76.26 ± 3.09	1489
I-04	3′-Cl-Ph	Et	H	0.0665 ± 0.0388	80.99 ± 0.38	1218
I-05	3′-F-Ph	Et	H	0.0348 ± 0.0206	71.99 ± 8.86	2069
I-06	3′-CF_3-Ph	Et	H	0.3016 ± 0.2135	34.42 ± 3.50	114
I-07	4′-Me-Ph	Et	H	0.0523 ± 0.0385	91.42 ± 1.90	1748
I-08	4′-Cl-Ph	Et	H	0.0178 ± 0.0112	83.86 ± 0.45	4711
I-09	4′-F-Ph	Et	H	0.0200 ± 0.0018	74.93 ± 4.82	3747
I-10	4′-MeO-Ph	Et	H	0.0232 ± 0.0071	>200	>8621
I-11	4′-OH-Ph	Et	H	0.0038 ± 0.0011	96.78 ± 8.17	25,468
I-12	4′-MeS-Ph	Et	H	0.0118 ± 0.0088	>200	>16,949
I-13	4′-$(CH_3)_2$CH-Ph	Et	H	0.1469 ± 0.0552	31.12 ± 3.81	212
I-14	3′,4′-diCl-Ph	Et	H	0.3102 ± 0.2008	75.35 ± 8.48	243
I-15	3′,4′-diF-Ph	Et	H	0.1617 ± 0.0371	86.43 ± 3.10	535
I-16	2′,4′-diMe-Ph	Et	H	0.4759 ± 0.4129	87.39 ± 1.87	184
I-17	2′,4′-diF-Ph	Et	H	0.0418 ± 0.0031	59.71 ± 8.78	1428
I-18	2′-N-pyridyl	Et	H	0.0228 ± 0.0017	79.44 ± 5.18	3484
I-19	H	Et	H	0.0334 ± 0.0056	75.01 ± 6.88	2246
I-20	Me	Et	H	0.0277 ± 0.0015	45.16 ± 10.71	1630
I-21	Cyclopropyl	Et	H	0.0245 ± 0.0027	47.19 ± 4.89	1926
I-22	$C(CH_3)_3$	Et	H	0.2965 ± 0.1034	67.93 ± 4.76	229
I-23	Ph	Et	Cl	0.0990 ± 0.0019	>200	>2020
I-24	3′-Me-Ph	Et	Cl	0.0860 ± 0.0152	77.10 ± 13.61	897
I-25	3′-Br-Ph	Et	Cl	0.1015 ± 0.0025	58.06 ± 9.84	572
I-26	3′-Cl-Ph	Et	Cl	0.0570 ± 0.0033	66.08 ± 31.43	1159
I-27	3′-F-Ph	Et	Cl	0.0713 ± 0.0436	>200	>2805
I-28	3′-CF_3-Ph	Et	Cl	0.1819 ± 0.0116	55.05 ± 3.82	303
I-29	4′-Me-Ph	Et	Cl	0.1380 ± 0.0469	>200	>1449
I-30	4′-Cl-Ph	Et	Cl	0.0893 ± 0.0629	>200	>2240
I-31	4′-F-Ph	Et	Cl	0.0181 ± 0.0017	64.92 ± 14.55	3587
I-32	3′,4′-diCl-Ph	Et	Cl	0.3495 ± 0.0197	190.20 ± 13.85	544
I-33	3′,4′-diF-Ph	Et	Cl	0.1512 ± 0.0960	115.43 ± 19.05	763
I-34	4′-MeO-3′-Cl-Ph	Et	Cl	0.1299 ± 0.0508	49.84 ± 8.21	384
I-35	Ph	CH_3	H	0.1865 ± 0.0936	54.62 ± 2.88	293
I-36	4′-MeO-Ph	CH_3	H	0.1941 ± 0.0103	66.88 ± 0.86	345
I-37	4′-F-Ph	CH_3	H	0.3552 ± 0.1654	42.23 ± 1.75	119
I-38	Ph	H	H	4.9825 ± 2.5257	79.06 ± 5.34	16
I-39	4′-MeO-Ph	H	H	3.9567 ± 2.0214	56.05 ± 0.89	14
I-40	4′-F-Ph	H	H	10.0751 ± 4.1284	61.62 ± 3.22	6
DB02	−	−	−	0.0067 ± 0.0021	>200	>29,851
ETR	−	−	−	0.0014 ± 0.0034	27.48 ± 5.69	19,628
NVP	−	−	−	0.0402 ± 0.0257	>200	>4975
AZT	−	−	−	0.0089 ± 0.0002	>200	>22,472

−Not applicable.

[a]All data represent as mean ± SD ($n = 3$).

[b]Effective concentration required to protect C8166 cell against the cytopathogenicity of HIV by 50%.

[c]Cytostatic concentration required to reduce C8166 cell proliferation by 50% tested by MTT method.

[d]Selectivity index: ratio CC_{50}/EC_{50}, a higher SI means a more selective compound.

10.0751 μmol/L respectively. Other 12 compounds (**I-01**, **I-05**, **I-08**, **I-09**, **I-10**, **I-11**, **I-12**, **I-18**, **I-20**, **I-21**, **I-22** and **I-31**) were found more potent than the reference drug NVP (EC_{50} = 0.0402 μmol/L) against HIV-1. The most potent compounds were **I-01** and **I-11** with EC_{50} values of 0.0068 and 0.0038 μmol/L, respectively. They were about 10 times more potent than NVP and were comparable with that observed with **DB02** (EC_{50} = 0.0067 μmol/L) and AZT (EC_{50} = 0.0089 μmol/L), but slightly lower than ETR (EC_{50} = 0.0014 μmol/L). Most compounds showed low to moderate cytotoxicity, and six compounds (**I-10, I-12, I-23**, **I-27**, **I-29** and **I-30**) out of them had CC_{50} > 200 μmol/L.

Based on above anti-HIV-1 results, preliminary SARs of these compounds could be delineated as the following. The side chain connected to C2 position of the pyrimidine ring is a major determinant for the anti-HIV-1 activity of DABOs. Obviously the (1*H*-pyrazol-3-yl)methyl-thio is favorable to the anti-HIV-1 activities. Compound **I-19** displayed an EC_{50} value of 0.0334 μmol/L which is similar to that of the reference drug NVP (0.0402 μmol/L). The diverse groups connecting to the C5′ position of the pyrazole ring are also studied. Changing from hydrogen (**I-19**) to Me and cyclopropyl gave compounds **I-20** and **I-21** similar EC_{50} value of 0.0277 and 0.0245 μmol/L respectively. However, replacing of the C5′ hydrogen of **I-19** with a *tert*-butyl decreased the activity for more than 10 folds (**I-22** *vs.* **I-19**). Substituting aryl at the C5′ position of the pyrazole ring could increase the activity against WT HIV-1 as those compounds which bearing phenyl group at the R_1 position displayed the most potent anti-HIV activity.

Furthermore, the SAR analysis of substitutions on the ω-phenyl of C2 side chain was explored. Compared with the non-substituted compound **I-01**, introduction of substituent to the phenyl ring seemed to be unfavorable to the HIV-1 inhibitory activities demonstrated by **I-02**−**I-34** activities. However, the exceptions were 4′-OH (**I-11**, EC_{50} = 0.0038 μmol/L, SI = 25,468) and 4′-SMe (**I-12**, EC_{50} = 0.0118 μmol/L, SI = 16,949) which enhanced the activities significantly and along with their low cytotoxicity, resulted in extremely high SI. In addition, the monosubstituted phenyl analogs were more potent than disubstituted derivatives (**I-2** and **I-13** *vs.* **I-14**−**I-17**). For monosubstituted compounds, the activity of *para*-substituted derivatives was slightly superior to that of *meta*-substituted derivatives, for example, **I-07**>**I-02**, **I-08**>**I-04**, **I-09**>**I-05**. Meanwhile, the nature of the substituent of the phenyl ring also influenced the antiviral activity of these novel *S*-DACOs, a clear order of C4′-substitution for anti-HIV activity was observed by direct comparison: OH (**I-11**, SI = 25,468)>SCH_3 (**I-12**, SI > 16,949)>H (**I-01**, SI = 12,424)>OCH_3 (**I-10**, SI > 8621)> Cl (**I-08**, SI = 4711)>F (**I-09**, SI = 3747)>Me (**I-07**, SI = 1748)>*i*Pr (**I-13**, SI = 212).

Since the introduction of a halogen atom to bioactive molecules could have significant influence on pharmaceutical profiles, the chlorine atom was also introduced to 4′-position (X substitution) of pyrazol ring to observe the effects on anti-HIV-1 activity. The results demonstrated that for some compounds, the inhibitory activities (EC_{50} values) against WT HIV-1 were marginally affected by the substitutions (H or Cl) at the 4′ position of the pyrazol nucleus. Through the pairwise comparison of the EC_{50} values, namely **I-02** (X = H, EC_{50} = 0.0739 μmol/L) and **I-24** (X = Cl, EC_{50} = 0.0860 μmol/L); **I-04** (X = H, EC_{50} = 0.0665 μmol/L) and **I-26** (X = Cl, EC_{50} = 0.0570 μmol/L); **I-06** (X = H, EC_{50} = 0.3016 μmol/L) and **I-28** (X = Cl, EC_{50} = 0.1819 μmol/L); **I-09** (X = H, EC_{50} = 0.0200 μmol/L) and **I-31** (X = Cl, EC_{50} = 0.0181 μmol/L); **I-14** (X = H, EC_{50} = 0.3102 μmol/L) and **I-32** (X = Cl, EC_{50} = 0.3495 μmol/L); **I-15** (X = H, EC_{50} = 0.1617 μmol/L) and **I-33** (X = Cl, EC_{50} = 0.1512 μmol/L), some compound's incorporation of a chlorine to C4′ position of pyrazol decreased the activity for more than 2−15 folds such as **I-23** *vs.* **I-01** (decreased 15 folds), **I-30** *vs.* **I-08** (decreased 5 folds), **I-27** *vs.* **I-05** and **I-29** *vs.* **I-07** (decreased 2 folds). Moreover, regarding the cytotoxicity of these compounds, some 4′-Cl substituted compounds (**I-23**, **I-30**, **I-27** and **I-29**) were much less toxic with the CC_{50} values higher than 200 μmol/L while the unsubstituted counterparts (**I-01**, **I-08**, **I-05** and **I-07**) had CC_{50} values ranging from 83 to 85 μmol/L. On the other hand, some unsubstituted compounds (**I-02, I-03**, **I-04** and **I-09**) have slightly higher CC_{50} values than their 4′-Cl substituted counterparts (**I-24**, **I-25**, **I-26** and **I-31**). Overall, average cytotoxicity of the 4′-Cl substituted compounds are lower than that of the unsubstituted compounds.

The previous SAR for *S*-DABOs indicated that the optimal moieties at positions 5 of the pyrimidine nucleus were dependent on the nature of the C2 and C6 side chain[25,26,31−33]. This series clearly showed that inhibitory activity increased proportionally with the modification of the C5 substituent in the order, H < Me < Et. As demonstrated, the 5-Et substituted derivatives (**I-10**, **I-09** and **I-01**) were 8−27-fold (SI ratio) more active than their 5-Me substituted counterparts (**I-36**, **I-37** and **I-35**), and 170−731-folds more active than their 5-H substituted counterparts (**I-39**, **I-40** and **I-38**). This confirmed that the steric bulkiness of C5 substituent is favored to maintain inhibitory activity against HIV-1 replication.

2.3. *In vitro anti-HIV-1 activity of **I-11** and **I-12***

Based on the results of the first round of screening, we performed further antiviral activity evaluation of **I-11** and **I-12** as representative compounds and assessed the activity against different HIV-1 strains including wild-type strains (HIV-1_{IIIB} and HIV-$1_{Ba\text{-}L}$), resistant strains (HIV-1_{A17}, HIV-1_{74V} and HIV-$1_{RF/V82F/184V}$) and clinical isolated strains (HIV-$1_{TC\text{-}1}$ and HIV-1_{WAN}). **DB02** and NVP were regarded as positive controls. The EC_{50}, CC_{50} and SI data are summarized in Table 2. As shown in the Table 2, **I-11** exhibited high potency antiviral replication against most test HIV-1 strains in different cells. In particular, the EC_{50} values of **I-11** against HIV-1_{IIIB}, HIV-$1_{Ba\text{-}L}$ and HIV-$1_{TC\text{-}1}$, the major isolates from high AIDS prevalence region in China were 0.0043, 0.0485 and 0.0145 μmol/L, respectively. These were about 5−14 times more potent than NVP (EC_{50} = 0.0274, 0.1659 and 0.1992 μmol/L, respectively) and were comparable to that observed with **DB02** (EC_{50} = 0.0095, 0.0377 and 0.0151 μmol/L, respectively). The antiviral effect of **I-12** is weaker and EC_{50} values ranging from 0.0189 to 0.2193 nmol/L. However, for HIV-1_{A17}, a multi-drug resistant strain of NNRTIs carrying the K103N and Y181C mutations, **I-11**, **I-12** and **DB02** all showed a significantly reduced inhibitory activity with EC_{50} values of 2.77, 4.87 and 6.01 μmol/L. Since the new generation of NNRTI, etravirine, showed a better inhibitory activity against K103N/Y181C double mutant HIV-1 strain (EC_{50}=0.050 μmol/L)[34], more improvements will be required to our compounds.

2.4. *HIV-1 reverse transcriptase activity assay*

Anti-RT activity of **I-11** and **I-12** were further evaluated by the enzymatic recombinant HIV-1 RT activity assay (Reverse transcriptase assay kit, Roche, Germany). While **I-11** showed similar

Table 2 Anti-HIV-1 activities of **I-11** and **I-12** against wild-type strains, clinical isolated strains, and resistant strains[a].

Strain	Cell	EC_{50} (μmol/L)				CC_{50} (μmol/L)				SI			
		I-11	I-12	DB02	NVP	I-11	I-12	DB02	NVP	I-11	I-12	DB02	NVP
HIV-1_{IIIB}	C8166	0.0043 ± 0.0023	0.0189 ± 0.0058	0.0095 ± 0.0017	0.0274 ± 0.0068	94.48 ± 2.40	>200	>200	>200	21,514	>10,582	>21,053	>7299
HIV-$1_{Ba\text{-}L}$	TZM-b1	0.0485 ± 0.0068	0.1933 ± 0.0261	0.0377 ± 0.0231	0.1659 ± 0.0465	77.10 ± 3.68	>200	>200	>200	1590	>1035	>5305	>1206
HIV-$1_{TC\text{-}1}$	PBMC	0.0145 ± 0.0001	0.0554 ± 0.0112	0.0118 ± 0.0006	0.1992 ± 0.0487	46.84 ± 5.20	>200	>200	>200	3230	>3610	>16,949	>1004
HIV-1_{WAN}	PBMC	0.0566 ± 0.0024	0.1651 ± 0.620	0.0151 ± 0.0025	0.0770 ± 0.0193	46.84 ± 5.20	>200	>200	>200	828	>1211	>13,245	>2597
HIV-1_{74V}[b]	C8166	0.0462 ± 0.0237	0.0881 ± 0.0179	0.0249 ± 0.0099	0.0768 ± 0.0193	94.48 ± 2.40	>200	>200	>200	2045	>2270	>8032	>2604
HIV-$1_{RF/V82F/I84V}$[c]	C8166	0.0541 ± 0.0231	0.2193 ± 0.0465	0.0465 ± 0.0089	0.0614 ± 0.0085	94.48 ± 2.40	>200	>200	>200	951	>912	>4301	>3257
HIV-1_{A17}[d]	C8166	2.77 ± 0.82	4.87 ± 2.71	6.01 ± 1.05	20.15 ± 3.10	94.48 ± 2.40	>200	>200	>200	34	>41	>33	>10

[a]Mean activity of EC_{50} was exhibited by mean ± SD, $n \geq 3$.
[b]Mutation site of HIV-$1_{RF/V82F/I84V}$ are V82F and M184V in protease encoding region in *pol* gene.
[c]Mutation site of HIV-1_{74V} is L74V in reverse transcriptase (RT) encoding region in *pol* gene.
[d]Mutation sites of HIV-1_{A17} are K103N and Y181C in RT encoding region in *pol* gene.

anti-RT activity (IC_{50} = 1.09 ± 0.59 μmol/L) with NVP (IC_{50} = 0.92 ± 0.09 μmol/L) but lower than that of **DB02** nearly three times (IC_{50} = 0.28 ± 0.03 μmol/L). **I-12** demonstrated lower inhibitory activity (2.27 ± 0.12 μmol/L). Both two compounds have similar dose-dependent pattern in inhibiting HIV-1 RT activity with NVP and **DB02** as showed in Fig. 2.

2.5. *In vivo pharmacokinetics study*

In vivo pharmacokinetic profile of compound **I-11** was examined in Sprague−Dawley rats (Table 3 and Fig. 3). As shown in Table 3 and Fig. 3, when administered at 5 mg/kg orally, compound **I-11** was rapidly absorbed with a T_{max} of 0.5 h, along with a half-life of 2.5 h and a mean residence time (MRT) of 0.554 h. The C_{max} of **I-11** was 654 ng/mL (1538 nmol/L), more than 400 times the EC_{50} value of anti-HIV-1 activity *in vitro* (Table 1). In this experiment, a 10.4% oral bioavailability of **I-11** was also observed.

2.6. *Molecular modeling analysis*

To better understand the structure-affinity relationship for this series of derivatives, the represent compounds **I-01**, **I-11**, **I-23**, **I-35**, **I-38** were docked into the NNRTIs binding pocket (NNIBP, PDB code: 1RT2) compared with **DB02** using the AutoDock4.2 program. Default parameters were used as described in the Sybyl-

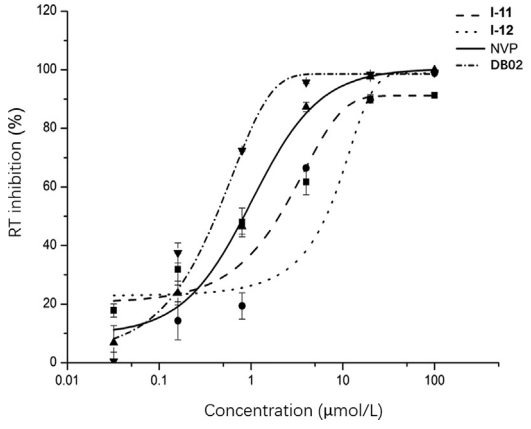

Figure 2 RT (reverse transcriptase) activity of **I-11**, **I-12**, **DB02** and NVP. The figure represents three independent experiments.

Table 3 Pharmacokinetic profile of **I-11**.

Parameter	i.v.[a]	Parameter	*p.o.*[b]
C_{max} (ng/mL)	7180	T_{max} (h)	0.500
$t_{1/2}$ (h)	1.20	C_{max} (ng/mL)	654
AUC_{last} (h·ng/mL)	2602	$t_{1/2}$ (h)	2.50
AUC_{INF} (h·ng/mL)	2629	AUC_{last} (h·ng/mL)	1302
MRT_{INF} (h)	0.554	AUC_{INF} (h·ng/mL)	1369
V_{ss} (L/kg)	0.213	V_Z/F (L/kg)	12.5
CL (L/h/kg)	0.384	CL/*F* (L/h/kg)	3.83
		F (%)	10.4

[a]Dosed intravenously at 1 mg/kg.
[b]Dosed orally at 5 mg/kg.

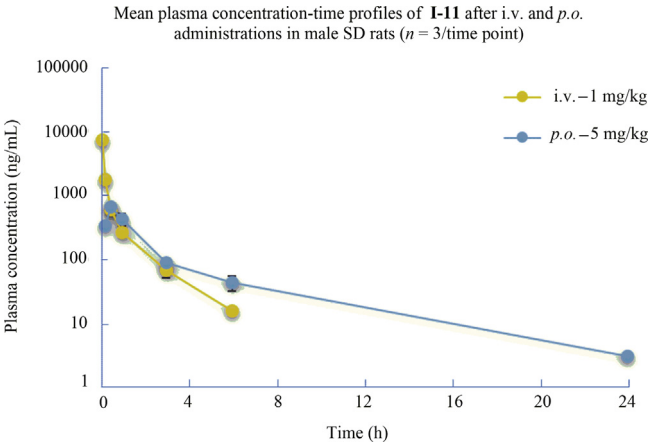

Figure 3 Plasma **I-11** concentration-time profiles in rats following *p.o.* administration (5 mg/kg) and i.v. administration (1 mg/kg).

2.0 manual unless otherwise specified and the result was displayed by MOE (Molecular Operating Environment). The proposed binding modes of these compounds to the NNIBP are shown in Figs. 4 and 5.

Binding mode of compound **I-11** in the allosteric site of HIV-1 WT RT in comparison with **DB02** was present at Fig. 4. Details are as follows: (1) the pyrimidine ring of **DB02** and **I-11** anchored into the same region of NNIBP through the H-bond formed between the 3-NH moiety on the pyrimidine ring and the main chain oxygen of Lys101. There also existed arene-H interaction between the pyrimidine ring of **I-11** and the polarized CH groups of Leu100. (2) The C2 side chain of the two compounds were well accommodated in the pocket surrounded by the side chains of Lys103, Val106, Pro236, Phe227 generating potential van der Waals' interactions and electrostatic interactions to give the advantage of the affinity between inhibitor and RT. In detail, the oxygen atom of C2-β-carbonyl of **DB02** and the nitrogen in the pyrazole ring of **I-11** made a hydrogen-bonding interaction with the N–H function of Lys103. When compared with **DB02**, one additional H-bond was observed between the NH in the pyrazole ring of **I-11** and the main chain oxygen of Lys103 which is good for the activity of compounds. Moreover, the terminal phenyl ring of **I-11** extended to the solvent exposure region which might be the main reason of diverse groups connecting to the C5′ position of the pyrazole ring are tolerant for this region. (3) The C6-ω-cyclohexyl group of **I-11** and **DB02** adopted the lowest energy "chair" conformation positing in the same hydrophobic sub-pocket and exhibiting hydrophobic interactions and van der Waals′ contacts with the aromatic amino acid residues Tyr181, Tyr188 and Trp229. Compared to **DB02**, the cyclohexyl group of **I-11** extended deeper into this region and formed arene-H with the indol ring of conserved amino acid Trp229 which might be the main reason of giving rise to the high-affinity binding to the NNBIP improving the anti-HIV-1 activity and prevented the loss of activity specifically caused by Y181C mutation.

The results of docking of **I-01**, **I-23**, **I-35** and **I-38** with the WT RT allosteric pocket provided additional explanation for the structure–activity relationship of these inhibitors (Fig. 5A–E). As can be seen from Fig. 5A, the interactions between compound **I-01** and RT were almost identical to those of compound **I-11** with RT, explains the fact that both **I-01** and **I-11** have good anti-HIV activity. Further analysis shows that the benzene rings at the end of C2 side chains of **I-01** and **I-11** reached the solvent-accessible region, the hydrophilic OH at the *para*-position of the benzene ring of compound **I-11** was undoubtedly more favorable for the activity than the hydrophobic aromatic hydrogen of **I-01**, resulting lower activity of **I-01**.

Introduction of a chlorine atom at the C4′ position of the pyrazole ring can be seen from the results in Table 1. For most compounds, it has little effect on the activity, excepted **I-23** with this value had been decreased significantly 15 folds, even though in the binding model **I-01** and **I-23** behaved similar (comparing Fig. 5A and B). It is worth noting that although no significant interaction between the chlorine atom and surrounding residues was observed in Fig. 5B, the introduction of a chlorine atom in compound **I-23** changed the relative position between pyrazole

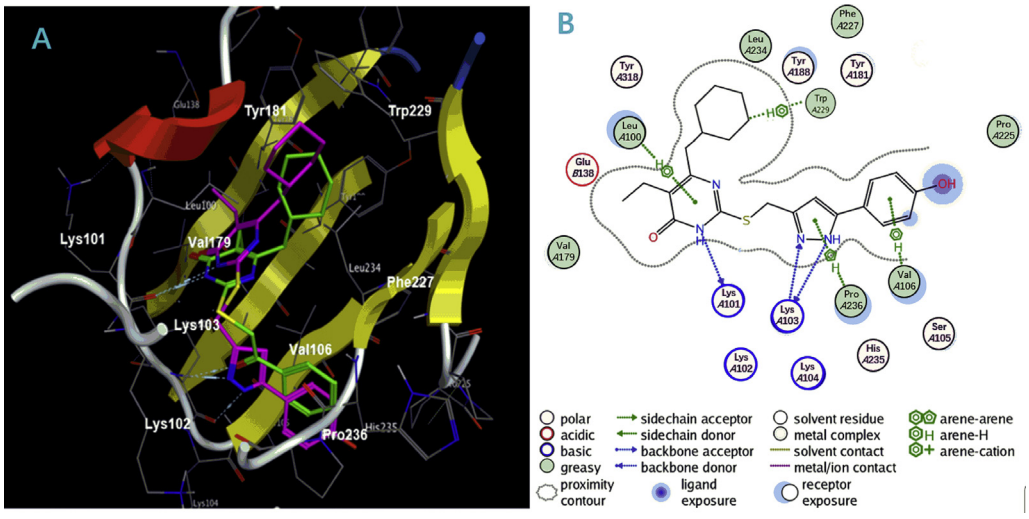

Figure 4 (A) Predicted binding mode of compound **I-11** (purplish red) in the allosteric site of HIV-1 wild-type (WT) RT (PDB code: 1RT2) in comparison with compound **DB02** (green); the docking results are showed by MOE (Molecular Operating Environment). The backbone is represented by ribbons, and amino acid residues important for binding interactions are labeled. Dotted lines show the interactions between HIV-1 RT and inhibitors. (B) The 2D-dimension representation of the interactions between the NNIBP and **I-11** is presented after the docking.

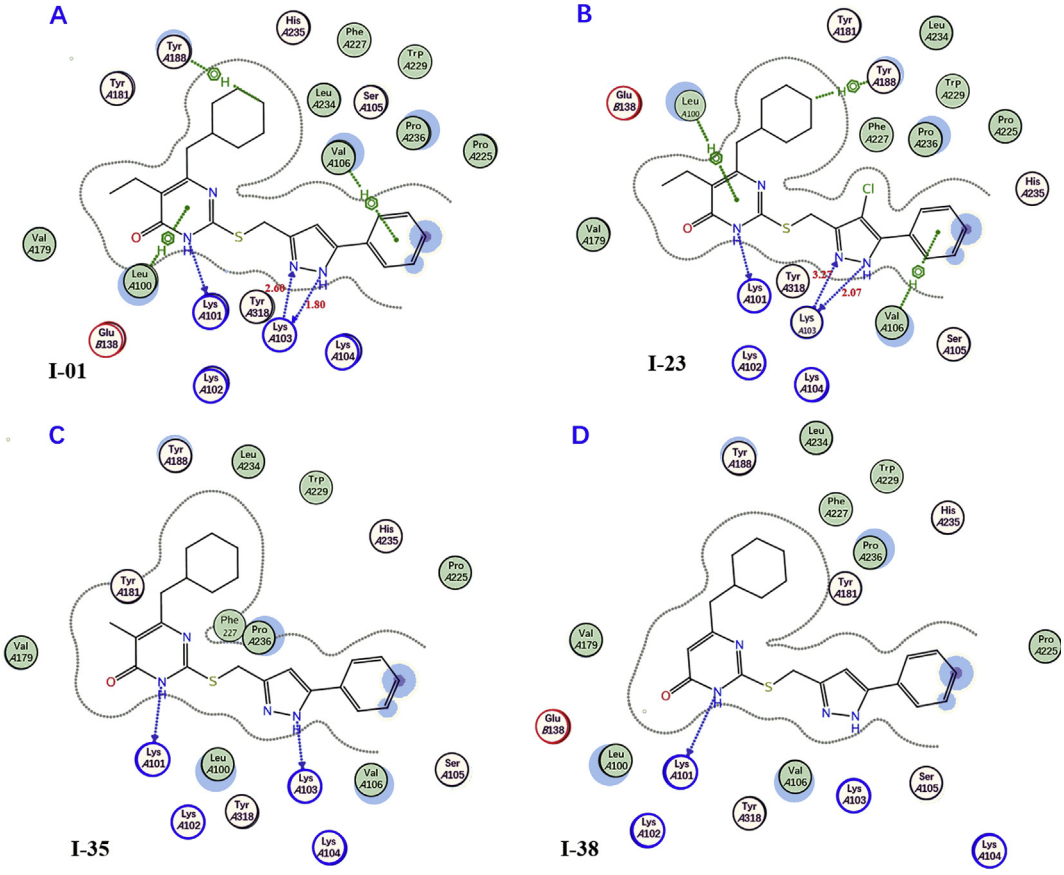

Figure 5 The 2D-dimension representation of the predicted binding modes of **I-01** (A), **I-23** (B)**, I-35** (C) and **I-38** (D) in the allosteric site of HIV-1 WT RT (PDB code: 1RT2).

ring and K103, thus affecting the strength of the hydrogen bond between them. The bond lengths of the two hydrogen bonds between the pyrazole ring of **I-23** and K103 are longer (2.07 and 3.27 Å respectively) than that on **I-01**—complex (1.80 and 2.60 Å respectively), providing a rational explanation of the reduced activity of **I-23**, and suggesting an important role of hydrogen-bonding interactions at this position.

In addition, the results of **I-35** and **I-38** docking with the allosteric pocket of WT RT (Fig. 5C and D) showed that the C5 substituent of the pyrimidine nucleus would make the inhibitor shift in NNBP, thus significantly affecting the formation of hydrogen bond between pyrazole ring and Lys103, which is considered to be important contributors to the binding affinity between RT inhibitors and enzymes. As shown in Fig. 5C, the introduction of a small methyl group at the C5 position of the pyrimidine ring (compound **I-35**) will move the pyrazole ring of the inhibitor to the left, cause losing the hydrogen bond between the nitrogen of pyrazole ring with the N−H of Lys103, as the result, the activity of **I-35** was reduced compared with that of **I-01**. Also, replace 5-Me with a smaller H would cause the two hydrogen bonds between the pyrazole ring of **I-38** and K103 disappeared simultaneously (Fig. 5D), which may be the reason why the efficacy of **I-38** against HIV-1 decreased sharply compared with that of **I-01**.

In summary, the results of the auto docking analysis provided support for the SARs elucidation of our newly designed and synthesized compounds. These facts will be considered in further *S*-DACOs analog structural design and optimization.

3. Conclusions

Based on the analysis of the ligand−receptor interactions, replacement of the C2-β-carbonyl fragment in the previously reported oxophenethyl-*S*-DACOs led structures with a pyrazol group resulting in the discovery of a novel series of potent NNRTIs. Most of these new congeners exhibited moderate to excellent activity against wild-type virus with an EC_{50} values ranging from 0.4759 to 0.0038 μmol/L. Selected compounds **I-11** and **I-12** displayed higher anti-HIV-1 activity against laboratory adapted strains and primary isolated strains including different subtypes and tropism strains. The results offer potential in further development of these compounds as a novel class of NNRTIs with improved antiviral efficacy and resistance profile. Furthermore, the selected compound **I-11** and **I-12** showed similar dose-dependent pattern in inhibiting HIV-1 RT activity with NVP confirming that the target of the compounds is RT. Compound **I-11** also displayed acceptable *in vivo* pharmacokinetic properties and bioavailability in rats. The preliminary SARs were discussed and the molecular simulation was performed. The docking study supported our initial hypothesis that the introduction of a pyrazolyl group at C2 position of pyrimidinone could provide an additional hydrogen bond with residue in NNIBP. In addition, the C6-cyclohexyl of these title compounds point to the indole side chain of the highly conserved W229 and forms an interesting CH−π interaction which showed vital importance in improving activity against a wide range of clinically relevant HIV-1 mutations. Hence the introduction of a large hydrophobic group at the

C6 position of the prymidine ring contributes to the development of new potent NNRTIs against mutant strains. Taking full advantage of the valuable information from SARs analysis, further optimization of this series of compounds aimed at improving drug resistance profiles and exploring the salient features controlling the activity are ongoing in our lab and will be reported in due course.

4. Experimental

4.1. Chemistry

Melting points (m.p.) were determined by a WRS-1 digital melting point instrument (Shanghai, China). ^{1}H NMR and ^{13}C NMR spectra were obtained on a Bruker AM 400/300 MHz spectrometer (Fällanden, Switzerland) using dimethyl sulfoxide-d_6 (DMSO-d_6) as solvent. Chemical shifts are reported in δ (ppm) units relative to the internal reference tetramethylsilane (TMS). Mass spectra were obtained on an Agilent LC/MSD TOF mass spectrometer (Watertown, MA, USA). The regents and solvents used were all of analytical grades, and were purified and dried by standard methods before use. All air-sensitive reactions were run under nitrogen stream protection. All the reactions were monitored by thin-layer chromatography (TLC) on pre-coated silica gel G plates at 254 nm under a UV lamp using ethyl acetate/petroleum ether as eluents. Flash chromatography separations were obtained on silica gel (300−400 mesh; Qingdao Marine Chemical Factory, Qingdao, China). 5-Alkyl-6-(cyclohexylmethyl)-2-thioxo-2,3-dihydropyrimidin-4(1*H*)-one (**4**) was prepared as previously reported[25,27].

4.1.1. Ethyl 2,4-dioxo-4-subtituted-butanoate (*6*)

Sodium metal (6.9 g, 3.0 mmol) was dissolved in absolute ethanol (40 mL). Diethyl oxalate (1.2 mmol) was added at 25 °C followed by a solution of appropriate methyl ketones **5** (1.0 mmol). The resulting mixture was stirred overnight at 25 °C. The reaction mixture was quenched by the addition of 1.0 mol/L HCl and extracted with EtOAc (2 × 40 mL). The combined organic layers were washed successively with water and brine and dried over $MgSO_4$. After filtration and concentration in vacuo, ethyl 2,4-dioxo-4-subtituted-butanoate (**6**) was obtained with yields of 88%−96% which can be used in the following step without further purification.

4.1.2. Ethyl 5-substituted-1H-pyrazole-3-carboxylate (*7*)

Hydrazine hydrate (1.5 mmol) was added to a solution of ethyl 2,4-dioxo-4-subtituted-butanoate (**6**) (1.0 mmol) in EtOH (30 mL) and the reaction mixture was refluxed for 3 h. The reaction mixture was cool to room temperature and the solvent was evaporated under reduced pressure. The residue was poured into 25 mL water and ethyl acetate for extraction, the organic layer was washed successively with water and brine, then dried over $MgSO_4$, filtered and concentrated in vacuo to give ethyl 5-substituted-1*H*-pyrazole-3-carboxylate (**7**) as a pale yellow solid with yields of 85%−90%, which can be used in the following step without further purification.

4.1.3. Ethyl 4-chloro-5-substituted-1H-pyrazole-3-carboxylate (*8*)

A solution of ethyl 5-substituted-1*H*-pyrazole-3-carboxylate (**7**) (1.0 mmol), *N*-chlorosuccinimide (NCS, 1.5 mmol) in CH_3CN/DMF (10 mL/2 mL) was heated to 55 °C for 20 h. The reaction mixture was concentrated under reduced pressure and the residue was poured into 25 mL of water and extracted by ethyl acetate. The organic layer was dried over $MgSO_4$, filtered and concentrated in vacuo to give ethyl 4-chloro-5-substituted-1*H*-pyrazole-3-carboxylate (**8**) as a light brown solid with yields of 40%−60%, which is used in the next step without further purification.

4.1.4. (4-Chloro-5-substituted-1H-pyrazol-3-yl)methanol (*9*)

$LiAlH_4$ (1.5 mmol) was added to a 0 °C solution of ester **7** or **8** (1.0 mmol) in drying THF (10 mL). The resultant mixture was stirred at 0 °C for 2 h. The reaction was quenched by the slow addition of saturate NH_4Cl. The aqueous layer was extracted with EtOAc and dried over $MgSO_4$. After filtration and concentration in vacuo, the residue was purified by flash column chromatography or recrystallization to give alcohol **9A** or **9B** as a white solid with the yield of 51%−78%.

4.1.5. 3-(Bromomethyl)-5-substituted-1H-pyrazole (*10*)

To a solution of alcohol **9** (1.0 mmol) in CH_3CN (10.0 mL) was added PBr_3 (1.5 mmol) slowly. The reaction was stirred at refluxing for 2 h. The reaction mixture was then cooled to room temperature and poured into the ice water and extracted with EtOAc (2 × 40 mL). The combined organic layers were washed successively with water and brine, dried over $MgSO_4$. After filtration and concentration in vacuo, the residue was purified by flash column chromatography to give 3-(bromomethyl)-4-chloro-5-substituted-1*H*-pyrazole (**10**) (92%−100%) as a white waxy solid.

4.1.6. 2-(((5-Substituted-1H-pyrazol-3-yl)methyl)thio)-6-(cyclohexylmethyl)-5-alkyl-pyrimidin-4 (3H)-one ***I*** (***1–40***)

K_2CO_3 (2.2 mmol) and compound **10** (2.2 mmol) were added to a solution of 2-thiouracil (**4**) (2 mmol) in anhydrous DMF (8 mL). The mixture was stirred at room temperature for 8−24 h. After TLC (EtOAc/PE) revealed the disappearance of the starting material, the reaction mixture was filtered. The suspension was then diluted with cold water and extracted with ethyl acetate. The combined organic extract was washed with brine, dried with Na_2SO_4, and evaporated to furnish crude product, which was purified by flash chromatography or by crystallization to give the pure target compounds **I** (**1–40**).

*4.1.6.1. 6-(Cyclohexylmethyl)-5-ethyl-2-(((5-phenyl-1H-pyrazol-3-yl)methyl)thio)pyrimidin-4(3H)-one (**I-01**).* White solid; Yield: 87.12%; m.p. 181−182 °C; ^{1}H NMR (400 MHz, $CDCl_3$, ppm) δ 0.85−0.88 (t, 3H, J = 8.1, CH_3), 0.97−1.00 (m, 2H, cyclohexyl-H), 1.07−1.12 (m, 3H, cyclohexyl-H), 1.65–1.69 (m, 5H, cyclohexyl-H), 1.82 (m, 1H, cyclohexyl-H), 2.46−2.48 (d, 2H, J = 6.9 Hz, CH_2-cyclohexyl), 2.51−2.53 (m, 2H, CH_2CH_3), 4.42 (s, 2H, CH_2-S), 6.52 (s, 1H, pyrazole-H), 7.34−7.36 (m, 3H, Ph-H), 7.67−7.69 (m, 2H, Ph-H), 10.24−10.73 (br, 1H, NH), 13.19 (br, 1H, NH); ^{13}C NMR (100 MHz, $CDCl_3$, ppm) δ 13.37, 18.75, 26.31 (2), 26.40, 26.90 (2), 33.36, 37.50, 41.80, 102.28, 122.74, 125.71 (2), 128.32, 128.86 (2), 130.56, 146.29, 146.99, 156.37, 163.11, 164.73; HR-MS: Calcd. for $C_{23}H_{28}N_4OS$ $[M+H]^+$: 409.2062, Found: 409.2057.

*4.1.6.2. 6-(Cyclohexylmethyl)-5-ethyl-2-(((5-(m-tolyl)-1H-pyrazol-3-yl)methyl)thio)pyrimidin-4(3H)-one (**I-02**).* White solid; Yield: 74%; m.p. 173−175 °C; ^{1}H NMR (400 MHz, DMSO-d_6,

ppm) δ 0.92 (m, 2H, cyclohexyl-H), 0.96−1.01 (t, 3H, J=6.9 Hz, CH_3), 1.08−1.14 (m, 3H, cyclohexyl-H), 1.53−1.60 (m, 5H, cyclohexyl-H), 1.80 (m, 1H, cyclohexyl-H), 2.30 (s, 3H, CH_3-Ph), 2.37−2.39 (m, 2H, CH_2-cyclohexyl), 2.37−2.39 (m, 2H, CH_2), 4.41 (s, 2H, CH_2-*S*), 6.55 (s, 1H, pyrazole-H), 7.06−7.09 (m, 1H, Ph-H), 7.23−7.28 (m, 1H, Ph-H), 7.50−7.54 (m, 2H, Ph-H), 12.79 (br, 2H, 2NH); ^{13}C NMR (100 MHz, DMSO-d_6, ppm) δ 13.18, 18.07, 20.92, 25.78 (3), 25.89 (2), 32.70, 36.62, 40.91, 101.48, 121.17, 122.11, 125.55, 128.31, 128.53, 130.87, 137.77, 145.19, 145.93, 156.32, 160.94, 162.91; HR-MS: Calcd. for $C_{24}H_{30}N_4OS$ $[M+H]^+$: 423.2219, Found: 423.2215.

*4.1.6.3. 2-(((5-(3-Bromophenyl)-1H-pyrazol-3-yl)methyl)thio)-6-(cyclohexylmethyl)-5-ethyl-pyrimidin-4(3H)-one (**I-03**).* White solid; Yield: 74%; m.p. 182−184 °C; ^{1}H NMR (400 MHz, $CDCl_3$, ppm) δ 0.89−0.91 (t, 3H, J=6.0 Hz, CH_3), 1.04 (m, 2H, cyclohexyl-H), 1.13 (m, 3H, cyclohexyl-H), 1.69 (m, 5H, cyclohexyl-H), 1.84 (m, 1H, cyclohexyl-H), 2.47−2.49 (m, 2H, CH_2-cyclohexyl), 2.51−2.54 (m, 2H, CH_2), 4.45 (s, 2H, CH_2S), 6.53 (s, 1H, pyrazole-H), 7.23−7.25 (m, 1H, Ph-H), 7.41−7.44 (m, 1H, Ph-H), 7.63−7.65 (m, 1H, Ph-H), 7.90 (m, 1H, Ph-H), 12.36 (br, 1H, NH), 13.19 (br, 1H, NH); ^{13}C NMR (100 MHz, $CDCl_3$, ppm) δ 13.38, 18.75, 26.32 (5), 33.38, 37.58, 41.90, 102.64, 122.64, 122.92, 124.29, 128.73, 130.29, 131.00, 133.49, 144.90, 147.13, 156.42, 163.40, 164.88; HR-MS: Calcd. for $C_{23}H_{27}BrN_4OS$ $[M+H]^+$: 487.1167, Found: 487.1163.

*4.1.6.4. 2-(((5-(3-Chlorophenyl)-1H-pyrazol-3-yl)methyl)thio)-6-(cyclohexylmethyl)-5-ethyl-pyrimidin-4(3H)-one (**I-04**).* White solid; Yield: 85%; m.p. 151−153 °C; ^{1}H NMR (400 MHz, $CDCl_3$, ppm) δ 0.97−1.01 (m, 2H, cyclohexyl-H), 1.01−1.12 (t, 3H, J = 7.2 Hz, CH_3), 1.17−1.21 (m, 3H, cyclohexyl-H), 1.65−1.69 (m, 5H, cyclohexyl-H), 1.80 (m, 1H, cyclohexyl-H), 2.47−2.49 (d, 2H, J = 6.6 Hz, CH_2-cyclohexyl), 2.51−2.54 (m, 2H, CH_2), 4.41 (s, 2H, CH_2-*S*), 6.50 (s, 1H, pyrazole-H), 7.25−7.30 (m, 2H, Ph-H), 7.56 (m, 1H, Ph-H), 7.58−7.70 (m, 1H, Ph-H), 12.56 (br, 1H, NH); ^{13}C NMR (100 MHz, $CDCl_3$, ppm) δ 3.36, 18.74, 26.13 (5), 33.37, 37.61, 41.92, 102.60, 122.69, 123.82, 125.86, 128.12, 130.05, 133.19, 134.73, 144.98, 147.21, 156.52, 163.40, 164.88; HR-MS: Calcd. for $C_{23}H_{27}ClN_4OS$ $[M+H]^+$: 443.1672, Found: 443.1670.

*4.1.6.5. 6-(Cyclohexylmethyl)-5-ethyl-2-(((5-(3-fluorophenyl)-1H-pyrazol-3-yl)methyl)thio)pyrimidin-4(3H)-one (**I-05**).* White solid; Yield: 74%; m.p. 159−161 °C; ^{1}H NMR (400 MHz, DMSO-d_6, ppm) δ 0.97−1.00 (m, 2H, cyclohexyl-H), 1.06−1.10 (t, 3H, J = 7.2 Hz, CH_3), 1.13−1.16 (m, 3H, cyclohexyl-H), 1.64−1.68 (m, 5H, cyclohexyl-H), 1.80 (m, 1H, cyclohexyl-H), 2.45−2.47 (m, 2H, CH_2-cyclohexyl), 2.47−2.51 (m, 2H, CH_2), 4.39 (s, 2H, CH_2-*S*), 6.49 (s, 1H, pyrazole-H), 6.96 (m, 1H, Ph-H), 7.28−7.46 (m, 3H, Ph-H), 12.40 (br, 2H, 2NH); ^{13}C NMR (75 MHz, DMSO-d_6, ppm) δ 13.32, 18.72, 26.30 (5), 33.37, 37.56, 41.90, 102.63, 112.64 (d, $^2J_{CF}$ = 22.6 Hz), 114.98 (d, J = 21.8), 121.33, 122.75, 130.36 (d, $^3J_{CF}$ = 8.1 Hz), 133.35 (d, $^3J_{CF}$ = 7.8 Hz), 145.29, 147.05, 156.25, 163.10 (d, $^1J_{CF}$ = 245.2 Hz), 163.32, 164.73; HR-MS: Calcd. for $C_{23}H_{27}FN_4OS$ $[M+H]^+$: 427.1968, Found: 427.1962.

*4.1.6.6. 6-(Cyclohexylmethyl)-5-ethyl-2-(((5-(3-(trifluoromethyl)phenyl)-1H-pyrazol-3-yl)methyl)thio)pyrimidin-4(3H)-one (**I-06**).* White solid; Yield: 68%; m.p. 162−164 °C; ^{1}H NMR (300 MHz, DMSO-d_6, ppm) δ 0.75 (m, 2H, cyclohexyl-H), 0.96−0.98 (t, 3H, J = 6.6 Hz, CH_3), 1.06 (m, 3H, cyclohexyl-H), 1.54 (m, 5H, cyclohexyl-H), 1.72 (m, 1H, cyclohexyl-H), 2.34−2.36 (m, 2H, cyclohexyl-H), 2.34−2.36 (m, 2H, CH_2), 4.42 (s, 2H, CH_2-S), 6.72 (s, CH, pyrazole-H), 7.59−7.60 (m, 2H, Ph-H), 8.01−8.0 (m, 2H, Ph-H), 12.58 (br, 2H, 2NH); ^{13}C NMR (75 MHz, DMSO-d_6, ppm) δ 13.12, 18.00, 24.94, 25.68 (2), 25.79 (2), 32.61, 36.56, 40.70, 102.09, 118.67, 121.10, 123.83, 124.08 (q, $^1J_{CF}$ = 270.6 Hz), 128.74, 129.63 (q, $^2J_{CF}$ = 31.3 Hz), 130.24, 132.89, 144.05, 146.06, 156.22, 160.68, 163.11; HR-MS: calcd. for $C_{24}H_{27}F_3N_4OS$ $[M+H]^+$: 477.1936, Found: 477.1932.

*4.1.6.7. 6-(Cyclohexylmethyl)-5-ethyl-2-(((5-(p-tolyl)-1H-pyrazol-3-yl)methyl)thio)pyrimidin-4(3H)-one (**I-07**).* White solid; Yield: 83%; m.p. 204−205 °C; ^{1}H NMR (400 MHz, DMSO-d_6, ppm) δ 0.96−1.00 (t, 3H, J = 6.9 Hz, CH_3), 1.11 (m, 5H, cyclohexyl-H), 1.59 (m, 5H, cyclohexyl-H), 1.80 (m, 1H, cyclohexyl-H), 2.28 (s, 3H, CH_3-Ph), 2.37−2.50 (m, 2H, cyclohexyl-H), 2.37−2.50 (m, 2H, CH_2), 4.39 (s, 2H, CH_2-*S*), 6.53 (s, 1H, pyrazole-H), 7.17−7.19 (m, 2H, Ph-H), 7.58−7.61 (m, 2H, Ph-H), 12.77 (br, 2H, 2NH); ^{13}C NMR (100 MHz, DMSO-d_6, ppm) δ 13.21, 18.05, 20.70, 25.77 (3), 25.88 (2), 32.70, 36.59, 40.89, 101.20, 121.16, 124.86 (2), 128.09, 129.23 (2), 137.01, 142.32, 145.67, 156.31, 160.94, 162.89.162.89; HR-MS: Calcd. for $C_{24}H_{30}N_4OS$ $[M+H]^+$: 423.2219, Found: 423.2217.

*4.1.6.8. 2-(((5-(4-Chlorophenyl)-1H-pyrazol-3-yl)methyl)thio)-6-(cyclohexylmethyl)-5-ethyl-pyrimidin-4(3H)-one (**I-08**).* White solid; Yield: 88%; m.p. 203−204 °C; ^{1}H NMR (400 MHz, DMSO-d_6, ppm) δ 0.97−0.99 (t, 3H, J = 7.2 Hz, CH_3), 1.09 (m, 2H, cyclohexyl-H), 1.18 (m, 3H, cyclohexyl-H), 1.57 (m, 5H, cyclohexyl-H), 1.75 (m, 1H, cyclohexyl-H), 2.35−2.39 (m, 2H, CH_2-cyclohexyl), 2.35−2.39 (m, 2H, CH_2), 4.39 (s, 2H, CH_2-*S*), 6.58−6.61 (s, 1H, pyrazole-H), 7.28−7.45 (m, 2H, Ph-H), 7.69−7.75 (m, 2H, Ph-H), 12.78 (br, 1H, NH); ^{13}C NMR (100 MHz, DMSO-d_6, ppm) δ 13.21, 18.03, 25.73 (2), 25.86 (3), 32.65, 36.58, 40.76, 101.71, 121.98, 124.93, 126.61, 127.66, 128.68, 131.86, 132.08, 145.91, 156.29, 160.85, 163.02; HR-MS: Calcd. for $C_{23}H_{27}ClN_4OS$ $[M+H]^+$: 443.1672, Found: 443.1668.

*4.1.6.9. 6-(Cyclohexylmethyl)-5-ethyl-2-(((5-(4-fluorophenyl)-1H-pyrazol-3-yl)methyl)thio)pyrimidin-4(3H)-one (**I-09**).* White solid; Yield: 89%; m.p. 174−176 °C. ^{1}H NMR (400 MHz, DMSO-d_6, ppm) δ 0.90 (m, 2H, cyclohexyl-H), 0.95−0.99 (t, 3H, J = 7.5 Hz, CH_3), 1.06−1.09 (m, 3H, cyclohexyl-H), 1.56−1.60 (m, 5H, cyclohexyl-H), 1.75 (m, 1H, cyclohexyl-H), 2.36−2.38 (m, 2H, CH_2-cyclohexyl), 2.36−2.38 (m, 2H, CH_2), 4.39 (s, 2H, CH_2-*S*), 6.57 (s, 1H, pyrazole-H), 7.18−7.24 (m, 2H, Ph-H), 7.73−7.77 (m, 2H, Ph-H), 12.78 (br, 1H, NH); ^{13}C NMR (DMSO-d_6, 75 MHz) δ 13.18, 18.02, 25.40 (2), 25.72, 25.85 (2), 32.65, 36.58, 40.71, 101.55, 115.53 (2C, d, $^2J_{CF}$ = 21.4 Hz), 121.07, 126.95 (2C, d, $^3J_{CF}$ = 8.0 Hz), 127.99, 144.42, 145.63, 156.32, 160.62, 161.64 (d, $^1J_{CF}$ = 243.0 Hz), 163.10; HR-MS: Calcd. for $C_{23}H_{27}FN_4OS$ $[M+H]^+$: 427.1968, Found: 427.1964.

*4.1.6.10. 6-(Cyclohexylmethyl)-5-ethyl-2-(((5-(4-methoxyphenyl)-1H-pyrazol-3-yl)methyl)thio)pyrimidin-4(3H)-one (**I-10**).* White solid; Yield: 50%; m.p. 283−284 °C; 1H NMR (400 MHz, DMSO-d_6, ppm) δ 0.95−1.00 (t, 3H, J = 7.2 Hz, CH_3), 1.02−1.12 (m, 2H, cyclohexyl-H), 1.16−1.20 (m, 3H, cyclohexyl-H), 1.59−1.62 (m, 5H, cyclohexyl-H), 1.78

(m, 1H, cyclohexyl-H), 2.36−2.38 (m, 2H, CH_2-cyclohexyl), 2.38−2.40 (m, 2H, CH_2), 3.76 (s, 3H, OCH_3), 4.37 (s, 2H, CH_2-*S*), 6.49 (s, 1H, pyrazole-H), 6.95−6.98 (m, 2H, Ph-H), 7.62−7.65 (m, 2H, Ph-H), 12.07−13.10 (br, 1H, NH); ^{13}C NMR (100 MHz, DMSO-d_6, ppm) δ 13.23, 18.02, 25.74 (2), 25.88 (3), 32.66, 36.58, 40.71, 55.06, 100.85, 114.11 (2), 121.10, 123.45, 126.31 (2), 142.23, 145.48, 156.39, 158.90, 160.65, 163.03; HR-MS: Calcd. for $C_{24}H_{30}N_4O_2S$ $[M+H]^+$: 439.2168, Found: 439.2164.

4.1.6.11. 6-(Cyclohexylmethyl)-5-ethyl-2-(((5-(4-hydroxyphenyl)-1H-pyrazol-3-yl)methyl)thio)pyrimidin-4(3H)-one ***(I-11).*** White solid; Yield: 54.59%; m.p. 228−230 °C; ^{1}H NMR (400 MHz, DMSO-d_6, ppm) δ 0.96−1.00 (t, 3H, J = 7.2 Hz, CH_3), 1.09−1.12 (m, 5H, cyclohexyl-H), 1.59−1.62 (m, 5H, cyclohexyl-H), 1.79 (m, 1H, cyclohexyl-H), 2.36−2.40 (m, 2H, CH_2-cyclohexyl), 2.36−2.40 (m, 2H, CH_2), 4.36 (s, 2H, CH_2-*S*), 6.42 (s, 1H, pyrazole-H), 6.78−6.81 (m, 2H, Ph-H), 7.50−7.53 (m, 2H, Ph-H), 9.62 (br, 1H, OH), 12.67 (br, 2H, 2NH); ^{13}C NMR (100 MHz, DMSO-d_6, ppm) δ 13.22, 18.04, 25.75, 25.88 (2), 26.07 (2), 32.67, 36.59, 40.76, 100.49, 115.48 (2), 121.42, 126.40 (2), 128.38, 145.64, 156.39, 157.25 (2), 160.82, 162.98; HR-MS: Calcd. for $C_{23}H_{28}N_4O_2S$ $[M+H]^+$: 425.2011, Found: 425.2008.

4.1.6.12. 6-(Cyclohexylmethyl)-5-ethyl-2-(((5-(4-(methylthio) phenyl)-1H-pyrazol-3-yl)methyl)thio)pyrimidin-4(3H)-one ***(I-12).*** White solid; Yield: 53%; m.p. 226−228 °C; ^{1}H NMR (400 MHz, DMSO-d_6, ppm) δ 0.96−1.00 (t, 3H, J = 7.2 Hz, CH_3), 1.08−1.10 (m, 2H, cyclohexyl-H), 1.15 (m, 3H, cyclohexyl-H), 1.58 (m, 5H, cyclohexyl-H), 1.78 (m, 1H, cyclohexyl-H), 2.37 (s, 3H, CH_3S), 2.46−2.50 (m, 2H, CH_2-cyclohexyl), 2.46−2.50 (m, 2H, CH_2), 4.40 (s, 2H, CH_2-*S*), 6.55 (s, 1H, pyrazole-H), 7.25−7.28 (m, 2H, Ph-H), 7.64−7.67 (m, 2H, Ph-H), 12.78 (br, 2H, 2NH); ^{13}C NMR (100 MHz, DMSO-d_6, ppm) δ 13.22, 14.52, 18.05, 25.77 (3), 25.89 (2), 32.69, 36.58, 40.88, 101.32, 121.15, 125.41 (2), 125.99 (2), 127.65, 137.69, 145.61, 156.25, 160.98, 162.90; HRMS (ESI-TOF): Calcd. for $C_{24}H_{30}N_4OS_2$ $[M+H]^+$: 455.1939, Found: 455.1935.

4.1.6.13. 6-(Cyclohexylmethyl)-5-ethyl-2-(((5-(4-isopropylphenyl)-1H-pyrazol-3-yl)methyl)thio)pyrimidin-4(3H)-one ***(I-13).*** White solid; Yield: 72%; m.p. 207−209 °C; ^{1}H NMR (400 MHz, DMSO-d_6, ppm) δ 0.92 (m, 2H, cyclohexyl-H), 0.96−1.01 (t, 3H, J = 7.5 Hz, CH_3), 1.08−1.10 (d, 6H, J = 7.5 Hz, $2CH_3$), 1.15−1.17 (m, 3H, cyclohexyl-H), 1.59 (m, 5H, cyclohexyl-H), 1.80 (m, 1H, cyclohexyl-H), 2.37−2.39 (m, 2H, CH_2-cyclohexyl), 2.37−2.39 (m, 2H, CH_2), 2.81−2.85 (m, 1H, $CHMe_2$), 4.40 (s, 2H, CH_2-*S*), 6.53 (s, 1H, pyrazole-H), 7.21−7.24 (m, 2H, Ph-H), 7.60−7.63 (m, 2H, Ph-H), 12.78 (br, 1H, NH); ^{13}C NMR (100 MHz, DMSO-d_6, ppm) δ 13.19, 18.06, 23.62 (2), 25.77 (3), 25.89, 25.89, 32.71, 33.16, 36.59, 40.92, 101.29, 121.15, 125.00 (2), 126.53 (2), 126.53, 128.49, 145.66, 147.92, 156.35, 160.92, 162.90; HR-MS: Calcd. for $C_{26}H_{34}N_4OS$ $[M+H]^+$: 451.2532, Found: 451.2529.

4.1.6.14. 6-(Cyclohexylmethyl)-2-(((5-(3,4-dichlorophenyl)-1H-pyrazol-3-yl)methyl)thio)-5-ethyl-pyrimidin-4(3H)-one ***(I-14).*** White solid; Yield: 52%; m.p. 309−311 °C; ^{1}H NMR (400 MHz, DMSO-d_6, ppm) δ 0.94 (m, 2H, cyclohexyl-H), 0.96−0.99 (t, 3H, J = 7.2 Hz, CH_3), 1.05−1.08 (m, 3H, cyclohexyl-H), 1.55−1.58 (m, 5H, cyclohexyl-H), 1.72 (m, 1H, cyclohexyl-H), 2.35−2.37 (m, 2H, CH_2-cyclohexyl), 2.35−2.37 (m, 2H, CH_2), 4.39 (s, 2H, CH_2-*S*), 6.68 (s, 1H, pyrazole-H), 7.59−7.62 (m, 1H, Ph-H), 7.68−7.72 (m, 1H, Ph-H), 7.94−7.95 (m, 1H, Ph-H), 12.81 (br, 2H, 2NH); ^{13}C NMR (100 MHz, DMSO-d_6, ppm) δ 13.19, 18.02, 24.90, 25.72 (2), 25.86 (2), 32.63, 36.58, 40.82, 102.26, 121.06, 124.96, 126.47 (2), 129.78, 130.82, 131.53, 141.48, 144.69, 156.09, 161.07, 162.99; HR-MS: Calcd. for $C_{23}H_{26}Cl_2N_4OS$ $[M+H]^+$: 477.1283, Found: 477.1279.

4.1.6.15. 6-(Cyclohexylmethyl)-2-(((5-(3,4-difluorophenyl)-1H-pyrazol-3-yl)methyl)thio)-5-ethyl-pyrimidin-4(3H)-one ***(I-15).*** White solid; Yield: 90%; m.p. 190−191 °C; ^{1}H NMR (300 MHz, DMSO-d_6, ppm) δ 0.94−0.99 (t, 3H, J = 7.2 Hz, CH_3), 1.05−1.08 (m, 5H, cyclohexyl-H), 1.55−1.59 (m, 5H, cyclohexyl-H), 1.72 (m, 1H, cyclohexyl-H), 2.32−2.38 (m, 2H, CH_2-cyclohexyl), 2.32−2.38 (m, 2H, CH_2), 4.38 (s, 2H, CH_2-*S*), 6.64 (s, 1H, pyrazole-H), 7.38−7.45 (m, 1H, Ph-H), 7.48−7.59 (m, 1H, Ph-H), 7.71−7.78 (m, 1H, Ph-H), 11.81−12.97 (br, 2H, 2NH); ^{13}C NMR (75 MHz, DMSO-d_6, ppm) δ 13.16, 18.01, 24.98, 25.70 (2), 25.84 (2), 32.62, 36.59, 40.71, 102.03, 113.8 (d, $^2J_{CF}$ = 18.2 Hz), 117.78 (d, $^2J_{CF}$ = 17.3 Hz), 121.04, 121.63, 129.61, 143.99, 145.48, 148.89 (dd, $^1J_{CF}$ = 244.5, $^2J_{CF}$ = 12.4 Hz), 149.72 (dd, $^1J_{CF}$ = 243.3, $^2J_{CF}$ = 12.3 Hz), 156.27, 160.66, 163.12; HR-MS: Calcd. for $C_{23}H_{26}F_2N_4OS$ $[M+H]^+$: 445.1874, Found: 445.1871.

4.1.6.16. 6-(Cyclohexylmethyl)-2-(((5-(2,4-dimethylphenyl)-1H-pyrazol-3-yl)methyl)thio)-5-ethyl-pyrimidin-4(3H)-one ***(I-16).*** White solid; Yield: 65%; m.p. 175−177 °C; ^{1}H NMR (DMSO-d_6, 400 MHz, ppm) δ 0.96−1.00 (m, 2H, cyclohexyl-H), 1.04−1.09 (t, 3H, J = 7.2 Hz, CH_3), 1.17−1.25 (m, 3H, cyclohexyl-H), 1.65 (m, 5H, cyclohexyl-H), 1.84 (m, 1H, cyclohexyl-H), 2.31 (s, 3H, CH_3-Ph), 2.35 (s, 3H, CH_3-Ph), 2.44−2.50 (m, 2H, CH_2-cyclohexyl), 2.44−2.50 (m, 2H, CH_2), 4.46 (s, 2H, CH_2-*S*), 6.35 (s, CH, pyrazole-H), 6.97−7.03 (m, 2H, Ph-H), 7.30−7.32 (m, 2H, Ph-H), 12.54 (br, 2H, NH); ^{13}C NMR (100 MHz, DMSO-d_6, ppm) δ 13.40, 18.77, 20.86, 21.23, 26.37, 26.50 (2), 27.51 (2), 33.43, 37.43,41.86, 105.16, 122.78, 126.82, 127.29, 129.03, 131.70, 135.80, 138.29, 145.35, 146.58, 156.26, 163.03, 164.67; HR-MS: Calcd. for $C_{25}H_{32}N_4OS$ $[M+H]^+$: 437.2375, Found: 437.2372.

4.1.6.17. 6-(Cyclohexylmethyl)-2-(((5-(2,4-difluorophenyl)-1H-pyrazol-3-yl)methyl)thio)-5-ethyl-pyrimidin-4(3H)-one ***(I-17).*** White solid; Yield: 75%; m.p. 207−209 °C; ^{1}H NMR (400 MHz, $CDCl_3$, ppm) δ 1.07−1.10 (m, 2H, cyclohexyl-H), 1.12−1.17 (t, 3H, J = 6.9 Hz, CH_3), 1.22−1.26 (m, 3H, cyclohexyl-H), 1.66−1.70 (m, 5H, cyclohexyl-H), 1.82 (m, 1H, cyclohexyl-H), 2.48−2.56 (m, 2H, CH_2-cyclohexyl), 2.48−2.56 (m, 2H, CH_2), 4.44 (s, 2H, CH_2-*S*), 6.62 (s, 1H, pyrazole-H), 6.85−6.92 (m, 2H, Ph-H), 7.76−7.7 (m, 1H, Ph-H), 12.09−12.42 (br, 2H, 2NH); ^{13}C NMR (75 MHz, $CDCl_3$, ppm) δ 13.33, 18.72, 26.29 (3), 26.38 (2), 33.36, 37.54, 41.90, 104.71 (dd, $^2J_{CF}$ = 17.5, 10.8 Hz), 111.90 (d, $^2J_{CF}$ = 21.2 Hz), 115.54 (d, $^2J_{CF}$ = 12.8 Hz), 122.75, 129.12, 141.28, 145.26, 156.33, 157.92, 159.67 (dd, $^1J_{CF}$ = 250.6 Hz, $^3J_{CF}$ = 11.8 Hz), 162.51 (dd, $^1J_{CF}$ = 248.8, $^3J_{CF}$ = 11.9 Hz), 163.22, 164.79; HR-MS: Calcd. for $C_{23}H_{26}F_2N_4OS$ $[M+H]^+$: 445.1874, Found: 445.1872.

4.1.6.18. 6-(Cyclohexylmethyl)-5-ethyl-2-(((5-(pyridin-2-yl)-1H-pyrazol-3-yl)methyl)thio)pyrimidin-4(3H)-one ***(I-18).*** White solid; Yield: 30%; m.p. 140−142 °C; ^{1}H NMR (400 MHz, $CDCl_3$,

ppm) δ 1.00−1.04 (m, 2H, cyclohexyl-H), 1.07−1.12 (t, 3H, J = 7.5 Hz, CH_3), 1.16−1.26 (m, 3H, cyclohexyl-H), 1.63−1.69 (m, 5H, cyclohexyl-H), 1.80−1.83 (m, 1H, cyclohexyl-H), 2.45−2.47 (d, 2H, J = 6.9 Hz, CH_2-cyclohexyl), 2.51−2.54 (m, 2H, CH_2), 4.49 (s, 2H, CH_2-*S*), 6.75 (s, 1H, pyrazole-H), 7.20−7.21 (m, 1H, pyridine-H), 7.69 (m, 2H, pyridine-H), 8.63−8.64 (m, 1H, pyridine-H), 10.27−10.67 (br, 2H, 2NH); ^{13}C NMR (100 MHz, $CDCl_3$, ppm) δ 13.32, 18.67, 26.28 (2), 26.39, 27.08, 27.08, 33.35, 37.38, 41.76, 101.19, 120.31, 122.69, 122.92, 137.01, 145.22, 147.74, 148.91, 149.41, 156.10, 161.87, 164.82; HR-MS: Calcd. for $C_{22}H_{27}N_5OS$ $[M+H]^+$: 410.2015, Found: 410.2012.

4.1.6.19. 2-(((1H-Pyrazol-3-yl)methyl)thio)-6-(cyclohexylmethyl)-5-ethylpyrimidin-4(3H)-one ***(I-19).*** White solid; Yield: 52%; m.p. 162−164 °C; ^{1}H NMR (400 MHz, $CDCl_3$, ppm) δ 1.05 (m, 2H, cyclohexyl-H), 1.07−1.12 (t, 3H, J = 7.5 Hz, CH_3), 1.17−1.26 (m, 3H, cyclohexyl-H), 1.66−1.70 (m, 5H, cyclohexyl-H), 1.80−1.85 (m, 1H, cyclohexyl-H), 2.45−2.47 (d, 2H, J = 7.2 Hz, CH_2-cyclohexyl), 2.51−2.53 (m, 2H, CH_2), 4.44 (s, 2H, CH_2-*S*), 6.27−6.28 (d, 1H, J = 7.5 Hz, pyrazole-H), 7.52−7.53 (d, J = 7.5 Hz, 1H, pyrazole-H), 10.90−10.95 (br, 2H, 2NH); ^{13}C NMR (100 MHz, $CDCl_3$, ppm) δ 13.28, 18.71, 26.31 (2), 26.41, 27.19 (2), 33.34, 37.36, 41.74, 104.76, 122.66, 131.71, 140.92, 145.81, 156.11, 163.09, 164.65; HR-MS: Calcd. for $C_{17}H_{24}N_4OS$ $[M+H]^+$: 333.1749, Found: 333.1747.

4.1.6.20. 6-(Cyclohexylmethyl)-5-ethyl-2-(((5-methyl-1H-pyrazol-3-yl)methyl)thio)pyrimidin-4(3H)-one ***(I-20).*** White solid; Yield: 49%; m.p. 175−176 °C; ^{1}H NMR (400 MHz, $CDCl_3$, ppm) δ 1.04 (m, 2H, cyclohexyl-H), 1.07−1.12 (t, 3H, J = 7.5 Hz, CH_3), 1.16−1.23 (m, 3H, cyclohexyl-H), 1.66−1.69 (m, 5H, cyclohexyl-H), 1.80−1.85 (m, 1H, cyclohexyl-H), 2.30 (s, 3H, CH_3-pyrazole), 2.44−2.46 (d, 2H, J = 7.2 Hz, CH_2-cyclohexyl), 2.50−2.53 (m, 2H, CH_2), 4.37 (s, 2H, CH_2-*S*), 6.02 (s, 1H, pyrazole-H), 11.01−11.45 (br, 2H, NH); ^{13}C NMR (100 MHz, $CDCl_3$, ppm) δ 11.48, 13.30, 18.68, 26.31, 26.31 (2), 27.33 (2), 33.33, 37.33, 41.72, 104.13, 122.59, 141.94, 146.81, 156.33, 163.02, 164.63; HR-MS: Calcd. for $C_{18}H_{26}N_4OS$ $[M+H]^+$: 347.1906, Found: 347.1904.

4.1.6.21. 6-(Cyclohexylmethyl)-2-(((5-cyclopropyl-1H-pyrazol-3-yl)methyl)thio)-5-ethyl-pyrimidin-4(3H)-one ***(I-21).*** White solid; Yield: 38%; m.p. 168−171 °C; ^{1}H NMR (400 MHz, $CDCl_3$, ppm) δ 1.04 (m, 2H, cyclohexyl-H), 1.07−1.12 (t, 3H, J = 7.5 Hz, CH_3), 1.17−1.20 (m, 4H, 2 × CH_2), 1.23−1.26 (m, 3H, cyclohexyl-H), 1.66−1.69 (m, 5H, cyclohexyl-H), 1.82 (m, 1H, cyclohexyl-H), 1.87−1.94 (m, 1H, cyclopropyl-H), 2.43−2.50 (d, 2H, J = 7.5 Hz, CH_2-cyclohexyl), 2.53−2.55 (m, 2H, CH_2), 4.36 (s, 2H, CH_2-*S*), 5.88 (s, 1H, pyrazole-H), 11.72 (br, 2H, NH); ^{13}C NMR (100 MHz, $CDCl_3$, ppm) δ 7.37, 7.87 (2), 13.31, 18.69, 26.32 (2), 26.43, 27.26 (2), 33.34, 37.36, 41.75, 100.94, 122.59, 146.25, 149.44, 156.37, 163.01, 164.63; HR-MS: Calcd. for $C_{20}H_{28}N_4OS$ $[M+H]^+$: 373.2062, Found: 373.2060.

4.1.6.22. 2-(((5-(tert-Butyl)-1H-pyrazol-3-yl)methyl)thio)-6-(cyclohexylmethyl)-5-ethyl-pyrimidin-4(3H)-one ***(I-22).*** White solid; Yield: 45%; m.p. 153−154 °C; ^{1}H NMR (400 MHz, $CDCl_3$, ppm) δ 0.85 (m, 2H, cyclohexyl-H), 1.02 (s, 9H, 3× CH_3), 1.07−1.12 (t, 3H, J = 7.5 Hz, CH_3), 1.34 (m, 1H, cyclohexyl-H), 1.67−1.71 (m, 7H, cyclohexyl-H), 1.84 (m, 1H, cyclohexyl-H), 2.44−2.47 (d, 2H, J = 6.9 Hz, CH_2-cyclohexyl), 2.51−2.56 (m, 2H, CH_2), 4.38 (s, 2H, CH_2-*S*), 6.05 (s, 1H, pyrazole-H), 12.68 (br, 2H, NH); ^{13}C NMR (100 MHz, $CDCl_3$, ppm) δ 13.32, 18.70, 26.34 (2), 26.44, 28.01 (2), 30.26 (3), 31.23, 33.35, 37.35, 41.76, 100.91, 122.76, 142.18, 146.33, 155.36, 156.21, 162.80, 164.32; HR-MS: Calcd. for $C_{21}H_{32}N_4OS$ $[M+H]^+$: 389.2375, Found: 389.2370.

4.1.6.23. 2-(((4-Chloro-5-phenyl-1H-pyrazol-3-yl)methyl)thio)-6-(cyclohexylmethyl)-5-ethyl-pyrimidin-4(3H)-one ***(I-23).*** White solid; Yield: 86%; m.p. 233−234 °C; ^{1}H NMR (400 MHz, DMSO-d_6, ppm) δ 0.94−0.97 (t, 3H, J = 7.2 Hz, CH_3), 0.99 (m, 2H, cyclohexyl-H), 1.06−1.08 (m, 3H, cyclohexyl-H), 1.56−1.59 (m, 5H, cyclohexyl-H), 1.81 (m, 1H, cyclohexyl-H), 2.32−2.34 (d, 2H, J = 6.0 Hz, CH_2-cyclohexyl), 2.36−2.38 (m, 2H, CH_2), 4.44 (s, 2H, CH_2-*S*), 7.40−7.51 (m, 3H, Ph-H), 7.77−7.79 (m, 2H, Ph-H), 10.88 (br, 1H, NH), 13.19 (br, 1H, NH); ^{13}C NMR (100 MHz, DMSO-d_6, ppm) δ 13.19, 18.01, 25.00 (2), 25.73 (2), 25.87, 32.63, 36.53, 40.76, 105.07, 121.05, 126.42, 126.42, 126.42, 128.67 (3), 140.28, 141.02, 155.86, 161.05, 162.92; HR-MS: Calcd. for $C_{23}H_{27}ClN_4OS$ $[M+H]^+$: 443.1672, Found: 443.1666.

4.1.6.24. 2-(((4-Chloro-5-(m-tolyl)-1H-pyrazol-3-yl)methyl)thio)-6-(cyclohexylmethyl)-5-ethyl-pyrimidin-4(3H)-one ***(I-24).*** White solid; Yield: 67%; m.p. 218−219 °C; ^{1}H NMR (400 MHz, DMSO-d_6, ppm) δ 0.89 (m, 2H, cyclohexyl-H), 0.95−0.99 (t, 3H, J = 7.2 Hz, CH_3), 1.08 (m, 3H, cyclohexyl-H), 1.56−1.59 (m, 5H, cyclohexyl-H), 1.79 (m, 1H, cyclohexyl-H), 2.30 (s, 3H, CH_3-Ph), 2.33−2.37 (m, 2H, CH_2-cyclohexyl), 2.33−2.37 (m, 2H, CH_2), 4.45 (s, 2H, CH_2-*S*), 7.17−7.19 (m, 1H, Ph-H), 7.31−7.36 (m, 1H, Ph-H), 7.57−7.59 (m, 2H, Ph-H), 12.95 (br, 2H, 2NH); ^{13}C NMR (100 MHz, DMSO-d_6, ppm) δ 13.16, 18.02, 20.97, 23.97, 25.76 (2), 25.90 (2), 32.67, 36.52, 40.79, 105.08, 121.10, 123.60, 126.98 (2), 128.52, 129.03, 137.81, 141.98, 142.53, 156.03, 161.03, 162.94; HR-MS: Calcd. for $C_{24}H_{29}ClN_4OS$ $[M+H]^+$: 457.1829, Found: 457.1826.

4.1.6.25. 2-(((5-(3-Bromophenyl)-4-chloro-1H-pyrazol-3-yl)methyl)thio)-6-(cyclohexylmethyl)-5-ethyl-pyrimidin-4(3H)-one ***(I-25).*** White solid; Yield: 90%; m.p. 236−237 °C; ^{1}H NMR (400 MHz, DMSO-d_6, ppm) δ 0.93−0.95 (t, 3H, J = 7.2 Hz, CH_3), 0.98 (m, 2H, cyclohexyl-H), 1.02−1.04 (m, 3H, cyclohexyl-H), 1.52−1.55 (m, 5H, cyclohexyl-H), 1.71 (m, 1H, cyclohexyl-H), 2.33−2.35 (m, 2H, CH_2-cyclohexyl), 2.33−2.35 (m, 2H, CH_2), 4.43 (s, 2H, CH_2-*S*), 7.42−7.45 (m, 1H, Ph-H), 7.55−7.58 (m, 1H, Ph-H), 7.80−7.82 (m, 1H, Ph-H), 7.95 (m, 1H, Ph-H), 13.01 (br, 2H, 2NH); ^{13}C NMR (100 MHz, DMSO-d_6, ppm) δ 13.58, 18.26, 23.13, 25.77 (4), 32.73, 36.87, 40.65, 104.93, 119.02, 121.85, 125.25, 128.74, 130.77 (2), 132.99, 140.95, 141.24, 160.40, 161.32, 168.14; HR-MS: Calcd. for $C_{23}H_{26}BrClN_4OS$ $[M+H]^+$: 521.0777, Found: 521.0773.

4.1.6.26. 2-(((4-Chloro-5-(3-chlorophenyl)-1H-pyrazol-3-yl)methyl)thio)-6-(cyclohexylmethyl)-5-ethyl-pyrimidin-4(3H)-one ***(I-26).*** White solid; Yield: 90.02%; m.p. 217−219 °C; ^{1}H NMR (400 MHz, DMSO-d_6, ppm) δ 0.88 (m, 2H, cyclohexyl-H), 0.93−0.98 (t, 3H, J = 7.2 Hz, CH_3), 1.03−1.05 (m, 3H,

cyclohexyl-H), 1.53−1.56 (m, 5H, cyclohexyl-H), 1.72 (m, 1H, cyclohexyl-H), 2.34−2.36 (m, 2H, CH_2-cyclohexyl), 2.34−2.36 (m, 2H, CH_2), 4.43 (s, 2H, CH_2-*S*), 7.44−7.53 (m, 2H, Ph-H), 7.76−7.81 (m, 2H, Ph-H), 12.50−13.54 (br, 2H, NH); ^{13}C NMR (100 MHz, DMSO-d_6, ppm) δ 13.26, 18.05, 23.37, 25.72 (2), 25.86 (2), 32.62 (2), 40.65, 105.34, 120.48, 124.85, 125.89, 128.02, 130.52, 131.97, 133.39, 140.52, 141.12, 157.09, 161.09, 164.33; HR-MS: Calcd. for $C_{23}H_{26}Cl_2N_4OS$ $[M+H]^+$: 477.1283, Found: 477.1279.

4.1.6.27. 2-(((4-Chloro-5-(3-fluorophenyl)-1H-pyrazol-3-yl) methyl)thio)-6-(cyclohexylmethyl)-5-ethyl-pyrimidin-4(3H)-one ***(I-27).*** White solid; Yield: 89%; m.p. 226−227 °C; ^{1}H NMR (300 MHz, DMSO-d_6, ppm) δ 0.95 (m, 3H, CH_3), 1.04 (m, 5H, cyclohexyl-H), 1.53 (m, 5H, cyclohexyl-H), 1.72 (m, 1H, cyclohexyl-H), 2.20−2.45 (m, 2H, CH_2-cyclohexyl), 2.20−2.45 (m, 2H, CH_2), 4.43 (s, 2H, CH_2-*S*), 7.22 (m, 1H, Ph-H), 7.55−7.65 (m, 3H, Ph-H), 12.98−13.05 (br, 2H, 2NH); ^{13}C NMR (75 MHz, DMSO-d_6, ppm) δ 13.15, 17.99, 23.55, 25.70 (2), 25.84 (2), 32.59, 36.52, 40.76, 105.46 (2), 112.88 (d, $^2J_{CF}$ = 22.9 Hz), 115.10 (d, $^2J_{CF}$ = 21.2 Hz), 121.10, 122.35 (2C), 130.77 (d, $^3J_{CF}$ = 7.7 Hz), 143.31, 155.95, 161.11, 162.12 (d, $^1J_{CF}$ = 242.2 Hz), 162.95; HR-MS: Calcd. for $C_{23}H_{26}ClFN_4OS$ $[M+H]^+$: 461.1578, Found: 461.1576.

4.1.6.28. 2-(((4-Chloro-5-(3-(trifluoromethyl)phenyl)-1H- pyrazol-3-yl)methyl)thio)-6-(cyclohexyl-methyl)-5-ethyl-pyrimidin-4(3H)-one ***(I-28).*** White solid; Yield: 64%; m.p. 198−199 °C; ^{1}H NMR (400 MHz, DMSO-d_6, ppm) δ 1.68−1.81 (m, 2H, cyclohexyl-H), 1.85−1.90 (t, 3H, J = 6.9 Hz, CH_3), 1.93 (m, 3H, cyclohexyl-H), 2.06−2.45 (m, 5H, cyclohexyl-H), 2.62 (m, 1H, cyclohexyl-H), 3.25−3.27 (m, 2H, cyclohexyl-H), 3.25−3.27 (m, 2H, CH_2), 5.37 (s, 2H, CH_2-*S*), 8.52−8.64 (m, 2H, Ph-H), 8.93−9.04 (m, 2H, Ph-H), 13.94 (br, 2H, 2NH); ^{13}C NMR (75 MHz, DMSO-d_6, ppm) δ 13.10, 17.98, 23.36, 25.66 (2), 25.79 (2), 32.58, 36.51, 40.76, 105.41, 105.54, 121.09, 122.58, 123.94 (q, $^1J_{CF}$ = 270.8 Hz), 124.66, 128.66, 129.33, 129.48 (q, $^2J_{CF}$ = 27.6 Hz), 129.79, 130.04, 155.81, 161.05, 162.95; HR-MS: Calcd. for $C_{24}H_{26}ClF_3N_4OS$ $[M+H]^+$: 511.1546, Found: 511.1545.

4.1.6.29. 2-(((4-Chloro-5-(p-tolyl)-1H-pyrazol-3-yl)methyl)thio)-6-(cyclohexylmethyl)-5-ethyl-pyrimidin-4(3H)-one ***(I-29).*** White solid; Yield: 63%; m.p. 225−226 °C; ^{1}H NMR (400 MHz, DMSO-d_6, ppm) δ 0.97−0.99 (m, 2H, cyclohexyl-H), 1.06−1.12 (t, 3H, J = 7.8 Hz, CH_3), 1.17 (m, 3H, cyclohexyl-H), 1.52−1.59 (m, 5H, cyclohexyl-H), 1.79 (m, 1H, cyclohexyl-H), 2.31 (s, 3H, CH_3-Ph), 2.35−2.37 (m, 2H, CH_2-cyclohexyl), 2.35−2.37 (m, 2H, CH_2), 4.44 (s, 2H, CH_2-*S*), 7.25−7.28 (m, 2H, Ph-H), 7.65−7.6 (m, 2H, Ph-H), 12.94 (br, 2H, 2NH); ^{13}C NMR (100 MHz, DMSO-d_6, ppm) δ 13.17, 18.00, 20.76, 24.04, 25.76 (2), 25.89 (2), 32.66, 36.51, 40.76, 104.82, 121.10, 126.68 (3), 129.22 (2), 137.95, 140.17, 141.01, 156.00, 161.02, 162.93; HR-MS: Calcd. for $C_{24}H_{29}ClN_4OS$ $[M+H]^+$: 457.1829, Found: 457.1826.

4.1.6.30. 2-(((4-Chloro-5-(4-chlorophenyl)-1H-pyrazol-3-yl) methyl)thio)-6-(cyclohexylmethyl)-5-ethyl-pyrimidin-4(3H)-one ***(I-30).*** White solid; Yield: 90%; m.p. 224−226 °C; ^{1}H NMR (400 MHz, DMSO-d_6, ppm) δ 0.88 (m, 2H, cyclohexyl-H), 0.93−0.98 (t, 3H, J = 7.2 Hz, CH_3), 1.03−1.05 (m, 3H, cyclohexyl-H), 1.53−1.56 (m, 5H, cyclohexyl-H), 1.74 (m, 1H, cyclohexyl-H), 2.34−2.36 (m, 2H, CH_2-cyclohexyl), 2.34−2.36 (m, 2H, CH_2), 4.43 (s, 2H, CH_2-*S*), 7.52−7.55 (m, 2H, Ph-H), 7.79−7.81 (m, 2H, Ph-H), 13.01 (br, 2H, 2NH); ^{13}C NMR (100 MHz, DMSO-d_6, ppm) δ 13.18, 17.99, 23.53, 25.71 (2), 25.85 (2), 32.60, 36.52, 40.75, 105.26, 121.09, 128.03 (3), 128.76 (2), 133.06, 140.46, 141.02, 155.78, 161.11, 162.93; HR-MS: Calcd. for $C_{23}H_{26}Cl_2N_4OS$ $[M+H]^+$: 477.1278, Found: 477.1275.

4.1.6.31. 2-(((4-Chloro-5-(4-fluorophenyl)-1H-pyrazol-3-yl) methyl)thio)-6-(cyclohexylmethyl)-5-ethyl-pyrimidin-4(3H)-one ***(I-31).*** White solid; Yield: 71%; m.p. 310−312 °C; ^{1}H NMR (400 MHz, DMSO-d_6, ppm) δ 0.96−0.98 (m, 2H, cyclohexyl-H), 1.04−1.06 (t, 3H, J = 7.8 Hz, CH_3), 1.13−1.15 (m, 3H, cyclohexyl-H), 1.50−1.58 (m, 5H, cyclohexyl-H), 1.75 (m, 1H, cyclohexyl-H), 2.35−2.37 (m, 2H, CH_2-cyclohexyl), 2.35−2.37 (m, 2H, CH_2), 4.43 (s, 2H, CH_2-*S*), 7.29−7.35 (m, 2H, Ph-H), 7.79−7.84 (m, 2H, Ph-H), 12.96 (br, 2H, 2NH); ^{13}C NMR (75 MHz, DMSO-d_6, ppm) δ 13.17, 17.99, 23.69, 25.72 (2), 25.86 (2), 32.61, 36.51, 40.75, 104.97 (2), 115.67 (2C, d, $^2J_{CF}$ = 21.5 Hz), 121.11, 125.93, 128.60 (2C, d, $^3J_{CF}$ = 8.2 Hz), 141.36, 155.92, 161.08, 161.96 (d, $^1J_{CF}$ = 244.7 Hz), 162.95; HR-MS: Calcd. for $C_{23}H_{26}ClFN_4OS$ $[M+H]^+$: 461.1578, Found: 461.1575.

4.1.6.32. 2-(((4-Chloro-5-(3,4-dichlorophenyl)-1H-pyrazol-3-yl)methyl)thio)-6-(cyclohexylmethyl)-5-ethyl-pyrimidin-4(3H)-one ***(I-32).*** White solid; Yield: 83%; m.p. 227−228 °C; ^{1}H NMR (400 MHz, DMSO-d_6, ppm) δ 0.93-0.98 (t, 3H, J = 7.2 Hz, CH_3), 1.04 (m, 5H, cyclohexyl-H), 1.53−1.55 (m, 5H, cyclohexyl-H), 1.70 (m, 1H, cyclohexyl-H), 2.33−2.36 (m, 2H, CH_2-cyclohexyl), 2.33−2.36 (m, 2H, CH_2), 4.42 (s, 2H, CH_2S), 7.46−7.55 (m, 2H, Ph-H), 7.98−7.99 (m, 1H, Ph-H), 12.72−13.36 (br, 2H, 2NH); ^{13}C NMR (100 MHz, DMSO-d_6, ppm) δ 13.17, 17.99, 23.17, 25.70 (2), 25.84 (2), 32.59, 36.52, 40.76, 105.57, 121.09, 124.86, 126.07, 128.73, 130.91, 131.49, 133.42, 140.68, 141.77, 155.74, 161.08, 162.96; HR-MS: Calcd. for $C_{23}H_{26}Cl_3N_4OS$ $[M+H]^+$: 511.0893, Found: 511.0890.

4.1.6.33. 2-(((4-Chloro-5-(3,4-difluorophenyl)-1H-pyrazol-3-yl) methyl)thio)-6-(cyclohexylmethyl)-5-ethyl-pyrimidin-4(3H)-one ***(I-33).*** White solid; Yield 69%; m.p. 228−229 °C; ^{1}H NMR (300 MHz, DMSO-d_6, ppm) δ 0.92−0.97 (t, 3H, J = 7.2 Hz, CH_3), 1.02−1.04 (m, 2H, cyclohexyl-H), 1.12−1.16 (m, 3H, cyclohexyl-H), 1.52−1.55 (m, 5H, cyclohexyl-H), 1.72 (m, 1H, cyclohexyl-H), 2.33−2.35 (m, 2H, CH_2-cyclohexyl), 2.33−2.35 (m, 2H, CH_2), 4.42 (s, 2H, CH_2-*S*), 7.51−7.57 (m, 1H, Ph-H), 7.64−7.73 (m, 1H, Ph-H), 7.73−7.80 (m, 1H, Ph-H), 13.00 (br, 2H, 2NH); ^{13}C NMR (75 MHz, DMSO-d_6, ppm) δ 13.12, 17.98, 23.26, 25.70 (2), 25.83 (2), 32.59, 36.52, 40.75, 105.29 (2), 115.24 (d, $^2J_{CF}$ = 18.8 Hz), 117.92 (d, $^2J_{CF}$ = 17.3 Hz), 121.10, 123.29 (2C), 147.84, 149.22 (dd, $^1J_{CF}$ = 245.8 Hz, $^2J_{CF}$ = 12.8 Hz), 149.38 (dd, $^1J_{CF}$ = 243.0 Hz, $^2J_{CF}$ = 12.8 Hz), 155.79, 161.07, 162.95. HR-MS: Calcd. for $C_{23}H_{25}ClF_2N_4OS$ $[M+H]^+$: 479.1484, Found: 479.1482.

4.1.6.34. 2-(((4-Chloro-5-(3-chloro-4-methoxyphenyl)-1H-pyrazol-3-yl)methyl)thio)-6-(cyclohexylmethyl)-5-ethyl-pyrimidin-4(3H)-one ***(I-34).*** White solid; Yield: 53%; m.p. 303−305 °C; ^{1}H NMR (400 MHz, DMSO-d_6, ppm) δ 0.88 (m, 2H, cyclohexyl-H), 0.93−0.98 (t, 3H, J = 6.9 Hz, CH_3), 1.04−1.07 (m, 3H, cyclohexyl-H), 1.54−1.57 (m, 5H, cyclohexyl-H), 1.74 (m, 1H,

cyclohexyl-H), 2.34−2.36 (m, 2H, CH_2-cyclohexyl), 2.34−2.36 (m, 2H, CH_2), 3.89 (s, 3H, OCH_3), 4.42 (s, 2H, CH_2-*S*), 7.24−7.27 (s, 1H, Ph-H), 7.72−7.81 (m, 2H, Ph-H), 12.52−13.21 (br, 2H, 2NH); ^{13}C NMR (100 MHz, DMSO-d_6, ppm) δ 13.18, 17.99, 23.71, 25.72 (2), 25.86 (2), 32.61, 36.52, 40.24, 56.15, 104.76, 112.91, 121.29, 123.5, 126.41, 127.59, 127.81, 154.49, 141.36, 142.55, 155.96, 160.95, 162.96; HR-MS: Calcd. for $C_{24}H_{28}Cl_2N_4O_2S$ $[M+H]^+$: 507.1388, Found: 507.1384.

*4.1.6.35. 6-(Cyclohexylmethyl)-5-methyl-2-(((5-phenyl-1H-pyrazol-3-yl)methyl)thio)pyrimidin-4(3H)-one (**I-35**).* White solid; Yield: 85%; m.p. 204−206 °C; ^{1}H NMR (400 MHz, DMSO-d_6, ppm) δ 0.94−1.00 (m, 2H, cyclohexyl-H), 1.08−1.11 (m, 3H, cyclohexyl-H), 1.58−1.73 (m, 6H, cyclohexyl-H), 1.87 (s, 3H, CH_3), 2.39−2.41 (d, 2H, J = 6.7 Hz, CH_2-cyclohexyl), 4.38 (s, 2H, CH_2-*S*), 6.59 (s, 1H, pyrazole-H), 7.28−7.30 (m, 1H, Ph-H), 7.36−7.41 (t, 2H, J = 7.2 Hz, Ph-H), 7.70−7.72 (d, 2H, Ph-H), 12.84 (br, 2H, 2NH); ^{13}C NMR (100 MHz, DMSO-d_6, ppm) δ 10.47, 25.67 (2), 25.87 (3), 32.61, 36.68, 41.49, 101.61, 115.07, 124.96 (2), 127.66 (2), 128.68, 131.03 (2), 156.20, 161.68,163.36; HR-MS: Calcd. for $C_{22}H_{26}N_4OS$ $[M+H]^+$: 395.1906, Found: 395.1903.

*4.1.6.36. 6-(Cyclohexylmethyl)-2-(((5-(4-methoxyphenyl)-1H-pyrazol-3-yl)methyl)thio)-5-methyl-pyrimidin-4(3H)-one (**I-36**).* White solid; Yield: 62%; m.p. 233−235 °C; ^{1}H NMR (400 MHz, DMSO-d_6, ppm) δ 0.95−0.99 (m, 2H, cyclohexyl-H), 1.11−1.13 (m, 3H, cyclohexyl-H), 1.59−1.63 (m, 6H, cyclohexyl-H), 1.88 (s, 3H, CH_3), 2.39−2.42 (m, 2H, CH_2-cyclohexyl), 3.77 (s, 3H, OCH_3), 4.36 (s, 2H, CH_2-*S*), 6.49 (s, 1H, pyrazole-H), 6.95−6.98 (m, 2H, Ph-H), 7.62−7.65 (m, 2H, Ph-H), 12.70 (br, 2H, 2NH); ^{13}C NMR (100 MHz, DMSO-d_6, ppm) δ 10.46, 25.68 (2), 25.89 (3), 32.61, 36.66, 41.46, 55.10, 100.90, 114.14 (2), 115.08, 123.60, 126.33 (2), 145.50, 156.23, 158.92, 161.54, 163.36; HR-MS: Calcd. for $C_{23}H_{28}N_4O_2S$ $[M+H]^+$: 425.2011, Found: 425.2009.

*4.1.6.37. 6-(Cyclohexylmethyl)-2-(((5-(4-fluorophenyl)-1H-pyrazol-3-yl)methyl)thio)-5-methyl-pyrimidin-4(3H)-one (**I-37**).* White solid; Yield: 87%; m.p. 186−188 °C; ^{1}H NMR (400 MHz, DMSO-d_6, ppm) δ 0.93−0.97 (m, 2H, cyclohexyl-H), 1.07−1.10 (m, 3H, cyclohexyl-H), 1.57−1.60 (m, 6H, cyclohexyl-H), 1.88 (s, 3H, CH_3), 2.38−2.41 (d, 2H, J = 6.9 Hz, CH_2-cyclohexyl), 4.38 (s, 2H, CH_2-*S*), 6.58 (s, 1H, pyrazole-H), 7.20−7.26 (m, 2H, J = 8.8 Hz, Ph-H), 7.73−7.77 (m, 2H, Ph-H), 12.77 (br, 1H, NH); ^{13}C NMR (100 MHz, DMSO-d_6, ppm) δ 10.97, 25.95, 26.18 (2), 26.37, 33.09 (2), 37.17, 41.98, 102.13, 116.08 (2C, d, $^2J_{CF}$ = 21.4 Hz), 125.44, 127.47 (2C, d, $^3J_{CF}$ = 8.1 Hz), 128.19, 129.21, 139.44, 149.38, 162.15 (d, $^1J_{CF}$ = 243.0 Hz), 162.17, 163.84. HR-MS: Calcd. for $C_{22}H_{25}FN_4OS$ $[M+H]^+$: 413.1811, Found: 413.1807.

*4.1.6.38. 6-(Cyclohexylmethyl)-2-(((5-phenyl-1H-pyrazol-3-yl)methyl)thio)pyrimidin-4(3H)-one (**I-38**).* White solid; Yield: 83%; m.p. 193−195 °C; ^{1}H NMR (400 MHz, DMSO-d_6, ppm) δ 0.89−0.97 (m, 2H, cyclohexyl-H), 1.09−1.17 (m, 3H, cyclohexyl-H), 1.58−1.62 (m, 6H, cyclohexyl-H), 2.32−2.34 (d, 2H, J = 6.93 Hz, CH_2-cyclohexyl), 4.40 (s, 2H, CH_2-S), 5.96 (s, 1H, pyrimidone-H), 6.61 (s, 1H, pyrazole-H), 7.27−7.32 (t, 1H, J = 7.3 Hz, Ph-H), 7.37−7.42 (t, 2H, J = 7.5 Hz, Ph-H), 7.70−7.72 (d, 2H, Ph-H), 12.80 (br, 2H, 2NH); ^{13}C NMR (100 MHz, DMSO-d_6, ppm) δ 25.24 (2), 25.87 (3C), 32.42, 36.15, 44.36, 101.74, 107.34, 124.94 (2), 127.73 (3), 128.73, 161.53, 163.53, 166.80; HR-MS: Calcd. for $C_{21}H_{24}N_4OS$ $[M+H]^+$: 381.1749, Found: 381.1747.

*4.1.6.39. 6-(Cyclohexylmethyl)-2-(((5-(4-methoxyphenyl)-1H-pyrazol-3-yl)methyl)thio)pyrimidin-4(3H)-one (**I-39**).* White solid; Yield: 47%; m.p. 184−186 °C; ^{1}H NMR (400 MHz, DMSO-d_6, ppm) δ 0.90−0.97 (m, 2H, cyclohexyl-H), 1.10−1.17 (m, 3H, cyclohexyl), 1.59−1.72 (m, 6H, cyclohexyl), 2.32−2.34 (d, 2H, J = 6.84 Hz, CH_2-cyclohexyl), 3.77 (s, 3H, OCH_3), 4.38 (s, 2H, CH_2-S), 5.96 (s, 1H, pyrimidone-H), 6.50 (s, 1H, pyrazole-H), 6.95−6.98 (d, 2H, J = 8.7 Hz, Ph-H), 7.62−7.65 (m, 2H, Ph-H), 12.72 (br, 2H, NH); ^{13}C NMR (100 MHz, DMSO-d_6, ppm) δ 25.55 (2), 25.87 (3), 32.43 (2), 36.13, 44.38, 55.08, 100.97, 107.36, 114.13 (2), 123.45, 126.32 (2), 145.47, 158.90 (2), 163.62, 166.72; HR-MS: Calcd. for $C_{22}H_{26}N_4O_2S$ $[M+H]^+$: 411.1855, Found: 411.1851.

*4.1.6.40. 6-(Cyclohexylmethyl)-2-(((5-(4-fluorophenyl)-1H-pyrazol-3-yl)methyl)thio)pyrimidin-4(3H)-one (**I-40**).* White solid; Yield: 89%; m.p. 203−205 °C. ^{1}H NMR (400 MHz, DMSO-d_6, ppm) δ 0.88−0.92 (m, 2H, cyclohexyl-H), 1.08−1.11 (m, 3H, cyclohexyl-H), 1.57−1.61 (m, 6H, cyclohexyl-H), 2.32−2.34 (d, 2H, J = 6.8 Hz, CH_2-cyclohexyl), 4.40 (s, 2H, CH_2-*S*), 5.96 (s, 1H, pyrimidone-H), 6.59 (s, 1H, pyrazole-H), 7.20−7.26 (m, 2H, Ph-H), 7.73−7.78 (m, 2H, Ph-H), 12.79 (br, 1H, NH); ^{13}C NMR (100 MHz, DMSO-d_6, ppm) δ 26.03 (2), 26.37, 32.92 (2), 36.65, 43.10, 44.86, 102.22, 105.54, 115.94 (d, $^2J_{CF}$ = 21.0 Hz), 116.10 (d, $^2J_{CF}$ = 21.5 Hz), 125.46, 127.49 (d, $^3J_{CF}$ = 8.1 Hz), 127.62 (d, $^3J_{CF}$ = 8.0 Hz), 129.68, 139.46, 149.38, 160.94, 162.28 (d, $^1J_{CF}$ = 242.8 Hz), 163.37; HR-MS: Calcd. for $C_{21}H_{23}FN_4OS$ $[M+H]^+$: 399.1655, Found: 399.1652.

4.2. Biology assay

4.2.1. Cells and viruses

C8166 and TZM-bl cells were kindly provided by the AIDS Reagent Project, the UK Medical Research Council (MRC). PBMCs were isolated by Ficoll-Hypaque method from whole blood collected from healthy donor. The C8166 cells and PBMCs were maintained at 37 °C in 5% CO_2 in RPMI-1640 medium supplemented with 10% heat-inactivating FBS (Gibco, Waltham, MA, USA). The TZM-bl cell was cultured in DMEM medium. In addition, wild-type strains HIV-1_{IIIB} and HIV-$1_{Ba\text{-}L}$, and HIV-1 resistant strains HIV-1_{A17}, HIV-1_{74V} and HIV-$1_{RF/V82F/184V}$ were obtained from the NIH AIDS Research and Reference Reagent Program (Bethesda, Maryland, ME, USA). Clinically isolated HIV strains, including HIV-$1_{TC\text{-}1}$ and HIV-1_{WAN} were isolated from AIDS patients without HAART in Yunnan, China.

4.2.2. Anti-HIV-1 activity assay

The antiviral assay based on the viral cytopathic effect (CPE) was performed on all compounds followed by cytotoxic detection by using MTT (3-(4,5-dimethyl-2-thiazolyl)-2,5-diphenyl-2-*H*-tetrazolium bromide, Thiazolyl Blue Tetrazolium Bromide) colorimetric reduction as previous reported[35]. Briefly, HIV-1_{IIIB},

C8166 cells and compounds were co-cultured for 3 days. The antiviral effect and cytotoxicity of each compound was analyzed by the inhibition of syncytia formation and the MTT assay. The EC_{50}, CC_{50} and SI were provided. The activity against different HIV-1 strains of the compounds with high SI was assessed by different detection system. The anti-HIV-$1_{Ba\text{-}L}$ activity was measured by a luciferase gene expression assay in TZM-bl cells as follows: cells (2×10^4 per well) and viruses were incubated in 96-well plates with a multiplicity of infection (MOI) of 0.1 in the presence or absence of serial dilutions of the test compound. After 3 days post-treatment, the luciferase activity was measured quantitatively by relative fluorescence units, using a Promega's luciferase activity assay system. The inhibitory activities against resistant and clinical strains were determined as previously described[36]. C8166 cells were infected with HIV-1_{A17}, HIV-1_{74V} or HIV-$1_{RF/V82F/184V}$, and PHA-stimulated PBMCs were incubated with HIV-1_{WAN} or HIV-$1_{TC\text{-}1}$ in RPMI-1640 at different serial dilutions of the compounds with a MOI of 0.1. Each assay included NVP as a positive control.

4.2.3. *In-vitro HIV-1 RT inhibitory assay*

Reverse transcriptase assay was performed using the Reverse Transcriptase Assay Kit (Roche, Mannheim, Germany) according to the manufacturer's instructions[26]. Briefly, the compounds **I-11** and **I-12** were dissolved in DMSO and stored at −4 °C. The compounds were then incubated with DIG-labeled reaction mixture at 37 °C for 2 h, then anti-DIG-POD solution was added, followed by substrate ABTS. Foscarnet was used as a positive control. The absorbency at 405 nm was read on Bio-Tek ELx 800 ELISA reader (Winooski, VT, USA)[37,38].

4.2.4. *Pharmacokinetics assays*

The mice used in this study were housed and handled strictly in accordance with the guidelines set by the Association for the Assessment and Accreditation of Laboratory Animal Care (Frederick, MD, USA). All animal experiments were conducted in accordance with the protocol approved by the Institutional Animal Care and Use Committee (IACUC) of Shanghai Chempartner Co., Ltd. Sample collection: six male Sprague−Dawley rats (200−230 g, 6−8 weeks) were divided into two groups ($n = 3$/group). Animals in group 1 received **I-11** i.v. at 1 mg/kg while animals in group 2 received **I-11** orally at 5 mg/kg (dissolved in 5% DMSO+5% Solutol HS 15 + 90% saline, strength: 0.5 mg/mL). Post-dosing serial blood samples (150 μL) were collected through tail vein into polypropylene tubes containing EDTA-K2 solutions as an anti-coagulant at 0.083, 0.25, 0.5, 1, 3, 6, 24 h (for i.v. arm) and 0.25, 0.5, 1, 3, 6, 24 h (for *p.o.* arm). Plasma was harvested by centrifuging the blood at 2000×*g* for 5 min and stored at approximately −70 °C until analysis.

LC−MS/MS method: LC−MS/MS system comprised an ACQUITY Ultra-performance liquid chromatography system (Waters, MA, USA) and a QTRAP-5500 mass spectrometer (AB Sciex Instruments) with an ESI ion source (Redwood city, CA, USA). The data acquisition and control system were created by using Analyst 1.5.1 software from AB SCIEX (Ontario, Canada). Chromatographic separation on an ACQUITY UPLC BEH C18 (2.1 mm×50 mm, 1.7 μm), mobile phase A (100% water containing 0.025% formic acid and 1 mmol/L ammonium acetate), mobile phase B (100% methanol containing 0.025% formic acid and 1 mmol/L ammonium acetate). The column was eluted at a flow rate of 0.6 mL/min in a gradient program consisting of 10% phase B (0−0.2 min), from 10% to 95% B (0.2−1.2 min), 95% B (1.20−1.60 min), from 95% to 10% B (1.60−1.61 min), 10% B (1.61−2 min). For **I-11**, the retention time for the analyte and IS (glipizide) were 1.46 min and 1.23 min respectively, injection volume is 0.5 μL. The precursor product ion pair was *m/z* 425.30 → 173.10 for **I-11**, *m/z* 446.20 → 321.10 for Diclofenac.

Standard curve preparation: Stock solution of **I-11** were prepared at 1 mg/mL in DMSO. The stock solution was diluted with MeOH:H_2O (7:3, *v/v*) to preparing serial working solution (20, 60, 200, 600, 2000, 6000, 20,000, 56,000, 60,000 ng/mL), 3 μL working solution was spiked into 57 μL male Sprague−Dawley rat plasma to obtain calibration standard curve (1, 2, 10, 30, 100, 300, 1000, 2700 and 3000 ng/mL).

Sample preparation: aliquot of 30 μL sample was added with 200 μL IS (glipizide, 20 ng/mL in ACN). The mixture was vortexed for 10 min at 750 rpm (Microporous Quick Shaker QB-9002, Changzhou, China) and centrifuged at 6000 rpm (Thermo Scientific Changzhou Multifuge X3R Centrifuge, Waltham, MA, USA) for 10 min. Aliquot of 0.5 μL supernatant was injected for LC−MS/MS analysis. For 10-fold diluted plasma samples, an aliquot of 3 μL plasma sample was diluted with 27 μL blank plasma, mixed well to achieve a dilution factor of 10. The subsequent processing procedure was the same as the un-diluted plasma samples.

4.3. *Molecular docking*

Molecular simulations were performed using AutoDock4.2 program[39]. All the molecules for docking were optimized for 5000-generation till the maximum derivative of energy became 0.005 kcal/mol·Å using the Tripos force field. Charges were computed and added according to Gasteiger-Huckel parameters. The published 3D crystal structure of the HIV-1 RT with TNK-651 complex was retrieved from the Protein Data Bank (PDB code: 1RT2). The molecules and proteins were prepared by using the AutoDockTools 1.5.4 (ADT). The bound ligand was extracted from the complexes, water molecules were removed, hydrogen atoms were automatically added, side chain amides and side chains bumps were fixed, and charges and atom types were assigned according to AMBER force field. Then, 100 separate docking calculations were performed using the reported modeling protocol[40].

Acknowledgments

Financial support from the National Natural Science Foundation of China (Grant No. U1702286, 21262044, 81660612, 21362017, 21762048). Program for Changjiang Scholars and Innovative Research Team in University (IRT_17R94, China). The Key Scientific and Technological Program of China (2017ZX09101004-014-007), The Yunnan Applicative and Basic Research Program (P0120150150, 2018FA048, China). Project of Innovative Research Team of Yunnan Province to Weilie Xiao. We thank Shanghai ChemPartner Co., Ltd. for completing the Pharmacokinetics Assays.

Author contributions

Yumeng Wu and Ruomei Rui carried out synthesis experiments. Chengrun Tang carried out anti-HIV evaluation experiments. Jiangyuan Wang carried out molecular simulation tests. Liumeng

Yang analyzed bioactivity data. Wei Ding and Yiming Li assisted with synthesis experiment. Christopher C. Lai assisted in spectral data analysis and manuscript correcting. Yueping Wang assisted with molecular simulation analysis. Ronghua Luo assisted in anti-HIV bioactivity experiments. Weilie Xiao analyzed pharmacokinetic data. Hongbing Zhang designed synthetic route and analyzed SAR. Yongtang Zheng designed bioactivity experiments. Yanping He designed overall the project and wrote manuscript.

Conflicts of interest

The authors have no conflicts of interest to declare.

Appendix A. Supporting information

Supporting information to this article can be found online at https://doi.org/10.1016/j.apsb.2019.08.009.

References

1. Esté JA, Cihlar T. Current status and challenges of antiretroviral research and therapy. *Antivir Res* 2010;**85**:25−33.
2. Margolis DM, Hazuda DJ. Combined approaches for HIV cure. *Curr Opin HIV AIDS* 2013;**8**:230−5.
3. Finzi D, Hermankova M, Pierson T, Carruth LM, Buck C, Chaisson RE, et al. Identification of a reservoir for HIV-1 in patients on highly active antiretroviral therapy. *Science* 1997;**278**:1295−300.
4. Chen X, Zhan P, Li D, de Clercq E, Liu X. Recent advances in DAPYs and related analogues as HIV-1 NNRTIs. *Curr Med Chem* 2011;**18**:359−76.
5. Blas-Garcia A, Esplugues JV, Apostolova N. Twenty years of HIV-1 non-nucleoside reverse transcriptase inhibitors: time to reevaluate their toxicity. *Curr Med Chem* 2011;**18**:2186−95.
6. Schrijvers R. Etravirine for the treatment of HIV/AIDS. *Expert Opin Pharmacother* 2013;**14**:1087−96.
7. Jackson A, McGowan I. Long-acting rilpivirine for HIV prevention. *Curr Opin HIV AIDS* 2015;**10**:253−7.
8. Wan ZY, Yao J, Mao TQ, Wang XL, Wang HF, Chen WX, et al. Pyrimidine sulfonylacetanilides with improved potency against key mutant viruses of HIV-1 by specific targeting of a highly conserved residue. *Eur J Med Chem* 2015;**102**:215−22.
9. Zhan P, Liu X, Li Z. Recent advances in the discovery and development of novel HIV-1 NNRTI platforms: 2006−2008 update. *Curr Med Chem* 2009;**16**:2876−89.
10. Song Y, Fang Z, Zhan P, Liu X. Recent advances in the discovery and development of novel HIV-1 NNRTI platforms (Part II): 2009−2013 update. *Curr Med Chem* 2014;**21**:329−55.
11. Zhan P, Liu X. Novel HIV-1 non-nucleoside reverse transcriptase inhibitors: a patent review (2005−2010). *Expert Opin Ther Pat* 2011;**21**:717−96.
12. Li D, Zhan P, de Clercq E, Liu X. Strategies for the design of HIV-1 non-nucleoside reverse transcriptase inhibitors: lessons from the development of seven representative paradigms. *J Med Chem* 2012;**55**:3595−613.
13. Zhan P, Pannecouque C, de Clercq E, Liu X. Anti-HIV drug discovery and development: current innovations and future trends. *J Med Chem* 2016;**59**:2849−78.
14. Artico M, Massa S, Mai A, Marongiu ME, Piras G, Tramontano E, et al. 3,4-Dihydro-2-alkoxy-6-benzyl-4-oxopyrimidines (DABOs): a new class of specific inhibitors of human immunodeficiency virus type 1. *Antiviral Chem Chemother* 1993;**4**:361−8.
15. D'cruz OJ, Uckun FM. Novel tight binding PETT, HEPT and DABO-based non-nucleoside inhibitors of HIV-1 reverse transcriptase. *J Enzyme Inhib Med Chem* 2006;**21**:329−50.
16. Mai A, Artico M, Sbardella G, Massa S, Novellino E, Greco G, et al. 5-Alkyl-2-(alkylthio)-6-(2,6-dihalophenylmethyl)-3,4-dihydropyrimidin-4(3*H*)-ones: novel potent and selective dihydro-alkoxy-benzyl-oxopyrimidine derivatives. *J Med Chem* 1999;**42**:619−27.
17. Nawrozkij MB, Rotili D, Tarantino D, Botta G, Eremiychuk AS, Musmuca I, et al. 5-Alkyl-6-benzyl-2-(2-oxo-2-phenylethylsulfanyl) pyrimidin-4(3*H*)-ones, a series of anti-HIV-1 agents of the dihydro-alkoxy-benzyl-oxopyrimidine family with peculiar structure-activity relationship profile. *J Med Chem* 2008;**51**:4641−52.
18. Wang YP, Chen FE, De Clercq E, Balzarini J, Pannecouque C. Synthesis and *in vitro* anti-HIV evaluation of a new series of 6-arylmethyl-substituted *S*-DABOs as potential non-nucleoside HIV-1 reverse transcriptase inhibitors. *Eur J Med Chem* 2009;**44**:1016−23.
19. Yang S, Chen FE, de Clercq E. Dihydro-alkoxyl-benzyl-oxopyrimidine derivatives (DABOs) as non-nucleoside reverse transcriptase inhibitors: an update review (2001−2011). *Curr Med Chem* 2012;**19**:152−62.
20. Yu M, Fan E, Wu J, Liu X. Recent advances in the DABOs family as potent HIV-1 non-nucleoside reverse transcriptase inhibitors. *Curr Med Chem* 2011;**18**:2376−85.
21. He Y, Chen F, Sun G, Wang Y, De Clercq E, Balzarini J, et al. 5-Alkyl-2-[(aryl and alkyloxylcarbonylmethyl)thio]-6-(1-naphthylmethyl) pyrimidin-4(3*H*)-ones as an unique HIV reverse transcriptase inhibitors of *S*-DABO series. *Bioorg Med Chem Lett* 2004;**14**:3173−6.
22. He Y, Chen F, Yu X, Wang Y, de Clercq E, Balzarini J, et al. Non-nucleoside HIV-1 reverse transcriptase inhibitors; Part 3. Synthesis and antiviral activity of 5-alkyl-2-[(aryl and alkyloxyl-carbonylmethyl)thio]-6-(1-naphthylmethyl) pyrimidin-4(3*H*)-ones. *Bioorg Chem* 2004;**32**:536−48.
23. Long J, Zhang DH, Zhang GH, Rao ZK, Wang YH, Tam SC, et al. The anti-HIV activity of three 2-alkylsulfanyl-6-benzyl-3,4-dihydropyrimidin-4(3*H*)-one derivatives acting as non-nucleoside reverse transcriptase inhibitor *in vitro*. *Acta Pharm Sin* 2010;**45**:228−34.
24. Rao ZK, Long J, Li C, Zhang SS, Zheng YT, He YP, et al. Synthesis and anti-HIV-1 activity of *S*-dihydro(alkyloxy)benzyloxypyrimidine derivatives. *Monatsh Chem* 2008;**139**:967−74.
25. He YP, Long J, Zhang SS, Li C, Lai CC, Zhang CS, et al. Synthesis and biological evaluation of novel dihydro-aryl/alkylsulfanyl-cyclohexylmethyl-oxopyrimidines (*S*-DACOs) as high active anti-HIV agents. *Bioorg Med Chem Lett* 2011;**21**:694−7.
26. Zhang XJ, Lu LH, Wang RR, Wang YP, Luo RH, Lai CC, et al. **DB-02**, a *C*-6-cyclohexylmethyl substituted pyrimidinone HIV-1 reverse transcriptase inhibitor with nanomolar activity, displays an improved sensitivity against K103N or Y181C than *S*-DABOs. *PLoS One* 2013;**11**:e81489.
27. Wu DC, Zhuang DM, Liu XF, Lu LH, Wang H, Li C, et al. Synthesis and biological evaluation of novel hydroxylphenethyl-*S*-DACOs as high active anti-HIV agents. *Lett Drug Des Discov* 2013;**10**:271−6.
28. Clay RJ, Collom TA, Karrick GL, Wemple J. A safe, economical method for the preparation of *β*-oxo esters. *Synthesis* 1993;**1993**:290−2.
29. Heller ST, Natarajan SR. 1,3-Diketones from acid chlorides and ketones: a rapid and general one-pot synthesis of pyrazoles. *Org Lett* 2006;**8**:2675−8.
30. Zhang J, Zhan P, Wu J, Li Z, Ge W, Pannecouque C, et al. Synthesis and biological evaluation of novel 5-alkyl-2-arylthio-6-((3,4-dihydroquinolin-1(2*H*)-yl)methyl)pyrimidin-4(3*H*)-ones as potent non-nucleoside HIV-1 reverse transcriptase inhibitors. *Bioorg Med Chem* 2011;**19**:4366−76.
31. Sbardella G, Mai A, Artico M, Massa S, Marceddu T, Vargiu L, et al. Does the 2-methylthiomethyl substituent really confer high anti-HIV-1 activity to *S*-DABOs?. *Med Chem Res* 2000;**10**:30−9.
32. Ji L, Chen FE, de Clercq E, Balzarini J, Pannecouque C. Synthesis and anti-HIV-1 activity evaluation of 5-alkyl-2-alkylthio-6-(arylcarbonyl or *α*-cyanoarylmethyl)-3,4-dihydropyrimidin-4(3*H*)-ones as novel non-nucleoside HIV-1 reverse transcriptase inhibitors. *J Med Chem* 2007;**50**:1778−86.
33. Rotili D, Tarantino D, Nawrozkij MB, Babushkin AS, Giorgia B, Marrocco B, et al. Exploring the role of 2 chloro-6-fluoro substitution

in 2-alkylthio-6-benzyl-5-alkylpyrimidin-4(3*H*)-ones: effects in HIV-1-infected cells and in HIV-1 reverse transcriptase enzymes. *J Med Chem* 2014;**57**:5212−25.
34. Huang B, Chen W, Zhao T, Li Z, Jiang X, Ginex T, et al. Exploiting the tolerant region I of the non-nucleoside reverse transcriptase inhibitor (NNRTI) binding pocket: discovery of potent diarylpyrimidine-typed HIV-1 NNRTIs against wild-type and E138K mutant virus with significantly improved water solubility and favorable safety profiles. *J Med Chem* 2019;**62**:2083−98.
35. Chander S, Tang CR, Penta A, Wang P, Bhagwat DP, Vanthuyne N, et al. Hit optimization studies of 3-hydroxy-indolin-2-one analogs as potential anti-HIV-1 agents. *Bioorg Chem* 2018;**79**:212−22.
36. Wang RR, Yang QH, Luo RH, Peng YM, Dai SX, Zhang XJ, et al. Azvudine, a novel nucleoside reverse transcriptase inhibitor showed good drug combination features and better inhibition on drug-resistant strains than lamivudine *in vitro*. *PLoS One* 2014;**9**:e105617.
37. Eberle J, Knopf CW. Nonisotopic assays of viral polymerases and related proteins. *Methods Enzymol* 1996;**275**:257−76.
38. Chander S, Wang P, Ashok P, Yang LM, Zheng YT, Murugesan S. Rational design, synthesis, anti-HIV-1 RT and antimicrobial activity of novel 3-(6-methoxy-3,4-dihydroquinolin-1(2*H*)-yl)-1-(piperazin-1-yl) propan-1-one derivatives. *Bioorg Chem* 2016;**67**:75−83.
39. Morris GM, Goodsell DS, Halliday RS, Huey R, Hart WE, Belew RK, et al. Automated docking using a Lamarckian genetic algorithm and an empirical binding free energy function. *J Comput Chem* 1998;**19**:1639−62.
40. Huey R, Morris GM, Olson AJ, Goodsell DS. A semiempirical free energy force field with charge-based desolvation. *J Comput Chem* 2007;**28**:1145−52.